Advances in Magnetics

Theory of Thermally Induced Phase Noise in Spin Torque Oscillators for a High-Symmetry Case

T. J. Silva and Mark W. Keller

National Institute of Standards and Technology, Boulder, CO 80305 USA

We derive equations for the phase noise spectrum of a spin torque oscillator in the macrospin approximation for the highly symmetric geometry where the equilibrium magnetization, applied field, anisotropy, and spin accumulation are all collinear. This particular problem is one that can be solved by analytical methods, but nevertheless illustrates several important general principles for phase noise in spin torque oscillators. In the limit, where the restoring torque is linearly proportional to the deviation of the precession amplitude from steady-state, the problem reduces to a sum of the Wiener-Lévy (W-L) and Ornstein-Uhlenbeck (O-U) processes familiar from the physics of random walks and Brownian motion. For typical device parameters, the O-U process dominates the phase noise and results in a phase noise spectrum that is nontrivial, with $1/\omega^2$ dependence at low Fourier frequencies, and $1/\omega^4$ dependence at high Fourier frequencies. The contribution to oscillator linewidth due to the O-U process in the low temperature limit is independent of magnetic anisotropy field H_k and scales inversely with the damping parameter, whereas in the high temperature limit the oscillator linewidth is independent of the damping parameter and scales as $\sqrt{|H_k|}$. Numerical integration of the fully nonlinear stochastic differential equations is used to determine the temperature and precession amplitude ranges over which our equations for phase noise and linewidth are valid. We then expand the theory to include effects of spin torque asymmetry. Given the lack of experimental data for nanopillars in the geometry considered here, we make a rough extrapolation to the case of nanocontacts, with reasonable agreement with published data. The theory does not yield any obvious means to reduce phase noise to levels required for practical applications in the geometry considered here.

Index Terms—**Langevin equations, macrospin, spin torque, spin torque oscillator, Ornstein-Uhlenbeck, Wiener-Lévy, phase noise.**

I. Introduction

SPIN TORQUE OSCILLATORS (STOs) are spintronic devices with potential applications in nanotechnology [1], [2]. When asymmetric spin currents drive sufficient angular momentum into an active ferromagnetic layer so as to overcome intrinsic damping in a current-perpendicular-to-plane giant-magnetoresistive (GMR) device, the magnetization of the layer can precess spontaneously [3]. The bias current and the GMR effect then result in an oscillating voltage output at frequencies ranging from radio-frequency (rf) to microwave.

As with any oscillator, one of the most important figures of merit is phase noise [4]. The first direct measurements of phase noise in an STO [5] showed a noise too large for applications such as telecommunications, though it could be significantly reduced by incorporating the STO in a phase-locked loop. These results highlight the need to understand the mechanisms behind phase noise in STOs, with the ultimate aim of reducing the noise to the point where practical applications become possible. To that end, we use ideas familiar from the analysis of other stochastic systems to consider here a particularly simple case where symmetry and uniformity permit a straightforward analysis of the equations of motion.

Manuscript received October 07, 2009; revised February 08, 2010; accepted February 22, 2010. Date of publication March 08, 2010; date of current version August 20, 2010. Corresponding author: T. J. Silva (e-mail: silva@boulder.nist.gov).

Color versions of one or more of the figures in this paper are available online at http://ieeexplore.ieee.org.

Digital Object Identifier 10.1109/TMAG.2010.2044583

We present a set of simple and easily interpreted predictive equations for the STO phase noise spectrum, provide detailed derivations for all of the results presented here, and demonstrate the need to assess the validity of these results. We find that the derived equations are valid only in the limit of sufficiently large amplitude excitations and sufficiently small temperature. A comparison of our analytical results with numerical simulations permits determination of the amplitude and temperature range over which the phase noise equations are valid.

The numerous treatments of STO phase noise in the literature [6]–[12] all begin by deriving Langevin equations for the dynamics of a macrospin in the presence of the effective thermal fluctuation field originally derived by W. F. Brown [13], where a Langevin equation is a stochastic differential equation (SDE) with an additive noise term [14]. These Langevin equations are presumably small amplitude expansions of model equations for the system, e.g., Landau-Lifshitz and the Slonczewski torque term, though the connection to such model equations is not explicitly derived. In addition, all these previous works focused on predictions of electrically measured linewidths in order to compare the theories with existing experimental data. Predictions of the spectral shape of the phase noise have rarely been reported, though it is generally presumed that the phase noise is diffusive in character, implying a $1/\omega^2$ dependence for the spectral density [6], [9].

References [6] and [8], in which quite different approaches are used, predict an inverse dependence of linewidth on precession amplitude, but they neglect the fact that STO frequency depends on precession amplitude. When this intrinsic nonlinear behavior is taken into account, as in the approach of [9] based on a small amplitude approximation, its contribution to the phase noise is significant. A treatment that avoids the small amplitude approximation, and includes the dependence of frequency on amplitude, has also been developed [15]. This novel approach makes use of a novel transformation of dynamic variables that precludes general expressions for the results in terms of measurable parameters, except at small amplitudes. Some general theoretical treatments of spin torque dynamics with thermal fluctuations rely upon solutions of the Fokker-Planck equation for a macrospin [16], [17]. So far, such methods have not yet been extended to make predictions of phase noise or linewidth in spin torque oscillators.

Motivated by the limitations discussed above, we present here a case where simple, analytical expressions for phase noise spectral density, and linewidth with appropriate restrictions, can be obtained directly from the Landau-Lifshitz-Slonczewski equation of motion for magnetization. We do this somewhat pedagogically, explaining in detail how thermal noise enters the problem and using several standard results from the theory of stochastic processes. The results are expressed in terms of physical quantities that can be independently determined by experiment, and we consider the range of precession amplitude and temperature over which the results are valid.

The following five fundamental assumptions are made as part of this theory. (1) We assume uniform magnetization. This is sometimes referred to as the "macrospin approximation." As such, we presume that this theory is strictly applicable only for the smallest nanopillar devices. Spectroscopic data combined with micromagnetic simulations suggest that devices with a characteristic diameter of 50 nm or less have properties resembling that of a true macrospin [18]. (2) We assume uniform effective magnetic fields. This essentially ignores the Oersted field that results from current flowing through the device. While simulations and theory suggest that the Oersted field can strongly affect dynamics in point-contact devices [19], [20], we expect that its role will be negligible in nanopillar devices in a saturating perpendicular magnetic field that are both sufficiently small to satisfy the macrospin approximation, and sufficiently efficient such that the dc current required to excite steady-state dynamics is minimal. (3) We assume that the Landau-Lifshitz (LL) equation is an adequate model for damped, gyromagnetic motion of the magnetization. Recently, there have been a variety of proposed alternative formulations of magnetization dynamics, including a model for nonlinear enhancement of scalar damping [21], the explicit inclusion of terms describing longitudinal relaxation of the microscopic magnetization vector [22], [23], and a tensor formulation for the damping parameter in metallic multilayers [24]. While we do not exclude the possibility that a model superior to LL for magnetization dynamics exists, we believe it necessary to formulate a theory of phase noise in terms of LL as an initial step; LL is the most rudimentary phenomenological model that is widely accepted as a reasonable approximation for magnetization dynamics in a variety of common experimental geometries. (4) We employ W. F. Brown's theory for the effective thermal fluctuation field acting on a macrospin based upon the analysis of Fokker-Planck equations derived from the LL equations [13]. We do not include the recently proposed spin-current fluctuation effect that may be a significant source of phase noise in spin torque oscillators at low temperatures [25]. (5) We assume that the Slonczewski model for spin torque in a nanopillar [26], including spin torque asymmetry, is sufficient for describing the salient aspects of spin torque relevant to the problem of phase noise. We do not include the effects of spin pumping [27] or of lateral spin diffusion [28]. We consider the former as a higher order correction for the types of effects described here, and the latter is ineffectual in the macrospin approximation.

The paper is organized as follows. In Section II, we provide a review of the standard model for thermal fluctuation stochastic parameters in magnetic systems, and present an explicit mathematical representation of thermal field fluctuations in terms of a stochastic train of impulse functions. In Section III, starting from the Landau-Lifshitz equation, with the addition of the Slonczewski torque term, we then derive a pair of coupled Langevin equations in the macrospin approximation. At this point, we break the problem into two parts, corresponding to thermal fluctuations in each of two orthogonal directions. In Section III-A, we calculate the phase noise for field fluctuations that cause direct phase jumps along the precession orbit, which occur on the time scale of the thermal field fluctuations. In Section III-B, we do the same for field fluctuations that cause deviations perpendicular to the precession orbit and result in phase deviations that occur on a time scale at which the system returns to steady-state after an energy perturbation. While the former case yields white frequency noise and thus permits a straightforward calculation of oscillator linewidth, the latter case does not. We describe the consequences of non-white frequency noise on the diffusion of the oscillator phase in Section IV. We modify our results for the case of spin torque asymmetry in Section VI. In Section VII, we compare our results with those in [9] and find that they agree for the particular high-symmetry geometry considered here. In Section VIII, we compare our analytical results with those obtained by directly integrating the full Langevin equation derived in Section III-B, permitting a quantitative determination of the temperature range over which the approximation of a linear restoring torque is valid. With some further approximations, we extend the analysis to the case of point-contacts in Section IX, and we conclude with a general discussion of the results in Section X. In the Appendix, we review the basic elements of the noise theory for linear systems and how it is applied for the case of phase noise.

II. Thermal Noise Model

In this section, we present the model for thermal noise in a magnetic system used throughout the rest of this paper, which includes both time domain and frequency domain representations of the thermal noise. We presume some familiarity on the part of the reader with the basic methods for the treatment of phase noise in linear systems. However, we have provided a brief review of the fundamental concepts in the Appendix.

We consider a uniformly magnetized "macrospin" of volume V subject to a random effective magnetic field $\boldsymbol{h}(t)$ arising from a stationary, Gaussian, white thermal noise source. Brown showed that the autocorrelation function $C_h(\tau)$ for such noise is given by [13] (where bold variables are used to indicate random processes)

$$\begin{aligned} C_h(\tau) &\doteq \langle \boldsymbol{h}(t)\boldsymbol{h}(t+\tau)\rangle \\ &= \frac{\alpha\omega_T}{[\gamma\mu_0]^2}\delta(\tau) \end{aligned} \tag{1}$$

where α is the dimensionless Landau-Lifshitz-Gilbert damping parameter, γ is the gyromagnetic ratio, μ_0 is the permeability of free space, ω_T is an effective thermal frequency defined as $\omega_T \doteq 2|\gamma|k_BT/M_sV, k_B$ is Boltzmann's constant, T is temperature, and M_s is the saturation magnetization density. The spectral density for the field noise is given by (see (99) in the Appendix)

$$\begin{aligned} S_h &= \int_{-\infty}^{+\infty} C_h(\tau)e^{-i\omega\tau}d\tau \\ &= \frac{\alpha\omega_T}{[\gamma\mu_0]^2}. \end{aligned} \tag{2}$$

For the sake of numerical simulations, we require a noise model that is consistent with (1) and (2) as limiting cases, but with a non-zero width autocorrelation function. We therefore modify the autocorrelation function to have the following form:

$$\hat{C}_h(\tau) \doteq \frac{\alpha\omega_T}{[\gamma\mu_0]^2}\hat{\delta}(\tau) \tag{3}$$

where $\hat{\delta}(t)$ is a continuous, smooth approximation to the Dirac delta function with a characteristic width Δt such that $\lim_{\Delta t\to 0}\hat{\delta}(t) = \delta(t)$, with the form $\hat{\delta}(t) = f(t)/\Delta t$, where $f(t)$ is a suitably representative pulse-like function centered at $t = 0$ with unity amplitude, and normalized such that $\int_{-\infty}^{+\infty} f(t)dt = \Delta t$. (In a formal mathematical sense, such a noise model is consistent with the so-called Stratonovich interpretation of stochastic differential equations in the limit of $\Delta t \to 0$, as opposed to the alternative Ito interpretation; see [14] and [29].) The spectral density for our realistic noise model is now given by

$$\hat{S}_h(\omega) = \frac{\alpha\omega_T}{[\gamma\mu_0]^2}F(\omega) \tag{4}$$

where $F(\omega)$ and $\hat{\delta(t)}$ are a Fourier transform pair, and $F(\omega) \cong 1$ for $\omega \ll 2\pi/\Delta t$.

Consistent with the previous two equations, we describe the noise as a chain of impulses of constant width Δt and random height $\boldsymbol{\delta H}$ that occur at random times with a mean rate λ. (A detailed description of the impulse model for thermal fluctuations may be found in [30] and [31].) As Brown did in deriving (1), we assume that the field pulse width Δt is much smaller than any other time scales in the problem. We can write the thermal noise waveform as

$$\boldsymbol{h}(t) = \Delta t \sum_{n=-\infty}^{+\infty} \boldsymbol{\delta H}_n \hat{\delta}(t - \boldsymbol{t}_n). \tag{5}$$

The field pulses are uncorrelated in time, and are therefore representative of a Poisson impulse process [31]. Since we model the noise as consisting of pulses of finite, albeit very short, time duration, we can now compute the variance of the magnetic field noise, with (3) and (4):

$$\begin{aligned} \langle \boldsymbol{h}^2\rangle &= \hat{C}_h(0) \\ &= \frac{S_h}{\Delta t}. \end{aligned} \tag{6}$$

From our model waveform for the field noise, (5), it is straightforward to compute the field noise variance as

$$\langle \boldsymbol{h}^2\rangle = \Delta t\lambda \left\langle \boldsymbol{\delta H}_n^2\right\rangle. \tag{7}$$

Combining (6) and (7), we obtain

$$\left\langle \boldsymbol{\delta H}_n^2\right\rangle = \frac{S_h}{\Delta t^2\lambda} \tag{8}$$

where the random pulse amplitude $\boldsymbol{\delta H}_n$ follows a Gaussian distribution.

III. Landau-Lifshitz-Slonczewski Langevin Equations

In this section, we present the essential math for spin torque oscillations of a macrospin subject to thermal fluctuations in the particular high-symmetry geometry where the applied field and anisotropy axes are collinear. We present the two basic integral equations for the time evolution of phase. Subsequently, there are two subsections, wherein we provide detailed analysis of the two integral equations in the limit of small temperature and/or large steady-state amplitude oscillations. We identify the first approximate equation as of the Wiener-Lévy (W-L) type. The second approximate equation can be reduced to the Ornstein-Uhlenbeck (O-U) form. Well-known methods exist for the solution of both equations. We then derive equations for the phase noise spectral density.

To start with, we consider the thermally perturbed dynamics for a macrospin of volume V with a net effective uniaxial anisotropy field H_k along the z-axis, excited by spin torque with the spin accumulation and the applied magnetic field H_0 along the same anisotropy direction. (The net anisotropy field includes all possible physical contributions to the anisotropy of the magnetization free energy, including, though not limited to, demagnetizing, magnetocrystalline, magnetoelastic, and interfacial/surface anisotropy effects.) Our stochastic form of the Landau-Lifshitz-Slonczewski (LLS) vector equation of motion is given by

$$\begin{aligned} \frac{d\overrightarrow{\boldsymbol{M}}}{dt} = -|\gamma|\mu_0\overrightarrow{\boldsymbol{M}} \times \overrightarrow{\boldsymbol{H}} - \frac{\alpha|\gamma|\mu_0}{M_s}\overrightarrow{\boldsymbol{M}} \times (\overrightarrow{\boldsymbol{M}} \times \overrightarrow{\boldsymbol{H}}) \\ + \frac{\beta(I)\,\omega_M}{M_s}\overrightarrow{\boldsymbol{M}} \times (\overrightarrow{\boldsymbol{M}} \times \hat{z}) \end{aligned} \tag{9}$$

where $\omega_M \doteq |\gamma|\mu_0 M_s, \beta(I) \doteq I\hbar\epsilon/2e\mu_0 M_s^2 V, I$ is the electric current, $\hbar$ is Planck's constant divided by $2\pi, e$ is the electron charge, and ϵ is the spin torque efficiency. A diagram of the considered geometry in spherical coordinates is presented

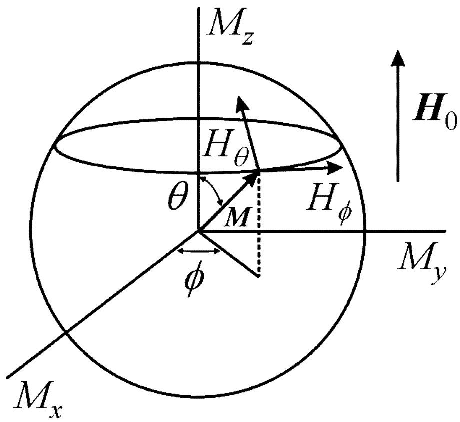

Fig. 1. Coordinate system for fields and magnetization.

in Fig. 1. In (9), $\vec{H}$ is the total effective field (including random variables), which can be written in spherical coordinates as

$$\begin{aligned}\vec{\boldsymbol{H}} &= -\frac{1}{\mu_0}\vec{\nabla}_M \boldsymbol{U} \\ &= -\frac{1}{\mu_0 M_s}\left(\frac{\partial \boldsymbol{U}}{\partial \theta}\hat{\theta} + \frac{1}{\sin\theta}\frac{\partial \boldsymbol{U}}{\partial \phi}\hat{\phi}\right) \\ &= \tilde{\boldsymbol{H}}_\theta\hat{\theta} + \tilde{\boldsymbol{H}}_\phi\hat{\phi}\end{aligned} \tag{10}$$

where $\boldsymbol{U}$ is the stochastic free energy of the macrospin.

We interpret the thermal fluctuations that give rise to random fluctuations in both the polar and azimuthal components of the effective field ($\tilde{\boldsymbol{H}}_\theta$ and $\tilde{\boldsymbol{H}}_\phi$) as arising from a temporally stochastic free energy function. Such a randomly varying energy surface gives rise to two components of the fluctuating magnetic field. The first, or "primary," component comes directly from the angular derivative of the instantaneous free energy function. These are the zero-mean field fluctuations described by our model in (5). A "secondary" component of randomly fluctuating effective field then results, because the trajectory of the magnetization is also fluctuating about steady-state, and the free energy is generally a function of the magnetization angle. The secondary fluctuating fields are not generally zero-mean.

Writing the total effective field in terms of both primary and secondary stochastic fields, we have

$$\vec{\boldsymbol{H}} = (\boldsymbol{H}_\theta + \boldsymbol{h}_\theta(t))\hat{\theta} + \boldsymbol{h}_\phi(t)\hat{\phi} \tag{11}$$

where $\boldsymbol{h}_\theta(t)$ and $\boldsymbol{h}_\phi(t)$ are the primary fluctuating thermal field components and $\boldsymbol{H}_\theta$ is the remaining non-zero secondary field component. From symmetry, $\boldsymbol{H}_\phi = 0$. For the present high-symmetry case, the secondary component of the stochastic effective field is simply

$$\boldsymbol{H}_\theta = -[H_0 + H_k\cos\boldsymbol{\theta}]\sin\boldsymbol{\theta} \tag{12}$$

where H_0 is the applied field. Note that for $H_k > 0$, the macrospin has an *easy axis* parallel to $\theta = 0$, whereas for $H_k < 0$, the macrospin has an *easy plane* orientation along $\theta = \pi/2$. If the macrospin in question is a nanopillar type device, an additional source of perpendicular anisotropy, (for example, interfacial anisotropy in magnetic multilayers) is required in order to have $H_k > 0$. In (12), we can see the essential difference between the secondary and primary components of the fluctuating field: The secondary field is the result of random fluctuations in the magnetization polar angle θ that are driven by the primary thermal fluctuation fields.

Continuing in our use of spherical coordinates, and ignoring primary thermal fluctuation terms that are proportional to the damping (because $\alpha \ll 1$ for magnetic materials of interest for spin torque applications) we can rewrite (9) as

$$\frac{d\boldsymbol{\phi}}{dt} = -|\gamma|\mu_0\frac{\boldsymbol{H}_\theta + \boldsymbol{h}_\theta(t)}{\sin\boldsymbol{\theta}} \tag{13}$$

$$\frac{d\boldsymbol{\theta}}{dt} = (\alpha|\gamma|\mu_0\boldsymbol{H}_\theta + \beta(I)\omega_M\sin\boldsymbol{\theta}) + |\gamma|\mu_0\boldsymbol{h}_\phi(t). \tag{14}$$

In general, (13) and (14) are coupled nonlinear SDEs. Our approach is to reduce the problem to that of two decoupled Langevin equations by linearization of the trigonometric factors, assuming small thermal fluctuations about a steady-state of arbitrarily large amplitude.

Since (14) does not depend on $\boldsymbol{\phi}$, it can be solved independently of (13). Substituting (12) into (14), we obtain

$$\begin{aligned}\frac{d\boldsymbol{\theta}}{dt} = |\gamma|\mu_0(\{-\alpha[H_0 + H_k\cos\boldsymbol{\theta}] \\ +\beta(I)M_s\}\sin\boldsymbol{\theta} + \boldsymbol{h}_\phi(t)).\end{aligned} \tag{15}$$

For $T = 0$, we calculate the time-average steady-state polar precession angle θ_0 by solving

$$\begin{aligned}0 &= \frac{d\theta}{dt} \\ &= (-\alpha[H_0 + H_k\cos\theta_0] + \beta(I)M_s)\sin\theta_0.\end{aligned} \tag{16}$$

Similarly, for $T = 0$, (13) reduces to the deterministic equation of motion

$$\frac{d\phi}{dt} = |\gamma|\mu_0[H_0 + H_k\cos\theta_0] \tag{17}$$

which has the solution $\phi = \Omega_0 t$, where $\Omega_0(\theta_0) \doteq -|\gamma|\mu_0[H_0 + H_k\cos\theta_0]$. Integration of the SDE in (13) for $T > 0$ yields a solution of the form

$$\boldsymbol{\phi}(t) = \Omega_0 t + [\boldsymbol{\phi}_1(t) + \boldsymbol{\phi}_2(t)] \tag{18}$$

where

$$\boldsymbol{\phi}_1(t) = -|\gamma|\mu_0\int_0^t \frac{\boldsymbol{h}_\theta(t')}{\sin(\boldsymbol{\theta}(t'))}\,dt' \tag{19}$$

$$\boldsymbol{\phi}_2(t) = |\gamma|\mu_0 H_k\int_0^t [\cos(\boldsymbol{\theta}(t')) - \cos(\theta_0)]\,dt' \tag{20}$$

and $\boldsymbol{\theta}(t)$ is the solution to (15). For (19) and (20), we have chosen to set $\boldsymbol{\phi}_1(0) = \boldsymbol{\phi}_2(0) = 0$ with no loss of generality.

Equation (19) describes a phase noise mechanism whereby thermal field fluctuations *perpendicular* to the precessional orbit cause "jumps" in the *phase* of the oscillator without any change in the amplitude of the precessional orbit. The characteristic time scale of the phase fluctuations is given by the duration of the field fluctuations themselves. Alternatively, (20) describes a process whereby thermal field fluctuations *parallel* to the precessional orbit cause fluctuations in the *amplitude* of precession, which then drive fluctuations in the precession frequency as a result of the dependence of frequency on amplitude. These resultant fluctuations have a characteristic time scale given by the restoration rate of the precession orbit back to steady-state after a thermal perturbation.

A. W-L Process

We can expand the denominator of (19) using both Taylor series and binomial expansions:

$$\boldsymbol{\phi}_1(t) \cong -|\gamma|\mu_0 \int_0^t \frac{\boldsymbol{h}_\theta(t')}{\sin(\theta_0)}(1+\cot\theta_0 \boldsymbol{\delta\theta}(t'))dt' \tag{21}$$

where $\boldsymbol{\theta}(t) = \theta_0 + \boldsymbol{\delta\theta}(t)$. We then assume $\boldsymbol{\delta\theta} \ll \theta_0$, (i.e., amplitude fluctuations are small relative to the precession amplitude), which implies $\boldsymbol{\delta\theta}(t) \ll \tan\theta_0$, and obtain the final approximate result

$$\boldsymbol{\phi}_1(t) = -\frac{|\gamma|\mu_0}{\sin(\theta_0)} \int_0^t \boldsymbol{h}_\theta(t')dt'. \tag{22}$$

Equation (22) is characteristic of a Wiener-Lévy (W-L) process, also known as the "random walk" used to describe Brownian motion when neglecting particle inertia [14]. Such stochastic processes are easily analyzed using a variety of conventional methods [14], [31]. Using standard theory for linear transformations of stochastic processes (see (112)–(117) in the Appendix) and the field noise spectral density in (2), we obtain the W-L contribution to the phase noise spectral density $S_\phi^{\mathrm{WL}}(\omega)$:

$$S_\phi^{\mathrm{WL}}(\omega) = \frac{\alpha\omega_T}{(m\omega)^2} \tag{23}$$

where $m \doteq \sin(\theta_0)$. The spectral density for the frequency noise is given by

$$S_\Omega^{\mathrm{WL}}(\omega) = \omega^2 S_\phi^{\mathrm{WL}}(\omega) \tag{24}$$

where the subscript refers to the average oscillator frequency Ω_0, in contrast to the Fourier frequency ω.

For the case of spectrally white frequency noise, the oscillator phase evolves as a diffusive random walk, with a mean square displacement (i.e., variance) that grows linearly in time

$$\langle \phi^2(t) \rangle = Dt \tag{25}$$

where D is the phase diffusion constant. (See the derivation of (121) in the Appendix for further details.) The line shape due to such a phase diffusion process is Lorentzian, with the full-width-at-half-maximum linewidth given by [30]

$$\Delta f = \frac{D}{2\pi}. \tag{26}$$

It can be shown that the spectral density of the frequency noise is equal to the phase diffusion constant, i.e., $D = S_\Omega$ [31]. Thus, the full-width-at-half-maximum (FWHM) linewidth due to this component of the phase noise is given by

$$\begin{aligned}\Delta f^{\mathrm{WL}} &= \frac{1}{2\pi} S_\Omega^{\mathrm{WL}}(\omega) \\ &= \frac{\alpha\omega_T}{2\pi m^2}.\end{aligned} \tag{27}$$

Using (27) with typical device parameters of $M_s = 800$ kA/m, $T = 300$ K, $V = 10^4$ nm^3, and $\alpha = 0.02$, and assuming maximum amplitude $m = 1$, the W-L contribution to the linewidth is $\Delta f^{\mathrm{WL}} \approx 600$ kHz.

B. O-U Process

The steady-state precession angle θ_0 is found using (16). For the case of an easy-plane anisotropy ($H_k < 0$), we obtain the solution

$$\theta_0 = 0 \quad \text{for } \beta(I) \le \alpha\left[\frac{H_0 + H_k}{M_s}\right] \tag{28}$$

$$\theta_0 = \arccos\left(\frac{\beta(I)M_S - \alpha H_0}{\alpha H_k}\right) \quad \text{for } \alpha\left[\frac{H_0+H_k}{M_s}\right] \le \beta(I) \le \alpha\left[\frac{H_0-H_k}{M_s}\right] \tag{29}$$

$$\theta_0 = \pi \quad \text{for } \beta(I) \ge \alpha\left[\frac{H_0 - H_k}{M_s}\right]. \tag{30}$$

For the case of an easy-axis anisotropy ($H_k > 0$), i.e., anisotropy perpendicular to the plane of a nanopillar device, steady-state precession is no longer a stable solution, with the result

$$\theta_0 = 0 \quad \text{for } \beta(I) < \alpha\left[\frac{H_0 - H_k}{M_s}\right] \tag{31}$$

$$\theta_0 = \pi \quad \text{for } \beta(I) \ge \alpha\left[\frac{H_0 - H_k}{M_s}\right]. \tag{32}$$

For the case of easy plane anisotropy and steady-state dynamics, we can now substitute (29) into (15) in order to obtain a differential equation for polar angle fluctuations about the steady-state:

$$\begin{aligned}\frac{d(\boldsymbol{\delta\theta})}{dt} = \frac{\alpha\omega_k}{2}&[\{\sin(2\theta_0)[\cos(\boldsymbol{\delta\theta}) - \cos(2\boldsymbol{\delta\theta})]\}. \\ &+ \{2\cos^2(\theta_0)\sin(\boldsymbol{\delta\theta}) - \cos(2\theta_0)\sin(2\boldsymbol{\delta\theta})\}] \\ &+ \gamma\mu_0 \boldsymbol{h}_\phi(t)\end{aligned} \tag{33}$$

where $\omega_k \doteq |\gamma|\mu_0 H_k$. (Note that (33) is applicable only in the case of steady-state dynamics, where (29) can be invoked. In the case where the current is too small to generate steady-state dynamics, as represented by (28), it is sufficient to solve (15) with $\theta_0 = 0$. More will be discussed about this at the end of this section.)

We particularly need to understand that (33) *is generally a nonlinear equation, which in the limit of large fluctuation angles can only be solved numerically*. This is a very important point that we shall expand upon in Section VIII. In the limit of small fluctuation angles $\boldsymbol{\delta\theta}$ relative to the steady-state angle θ_0, one can linearize (33) and obtain

$$\frac{d(\boldsymbol{\delta\theta})}{dt} \cong \eta\boldsymbol{\delta\theta} + |\gamma|\mu_0 \boldsymbol{h}_\phi(t) \tag{34}$$

where $\eta \doteq \alpha\omega_k \sin^2\theta_0$. In physical terms, η is the restoration rate for the mode, i.e., the rate at which the mode returns to steady-state once it has been perturbed by a thermal fluctuation. Equation (34) is an example of an Ornstein-Uhlenbeck (O-U) process, which has been thoroughly analyzed in the context of Brownian motion and Johnson noise [32], [33].

The limits to the applicability of the small angle approximation used to derive (34) can be clearly seen by expanding (33) to third order in both $\delta\theta$ and θ_0, assuming $\delta\theta \ll 1$ and $\theta_0 \ll 1$:

$$\frac{d(\boldsymbol{\delta\theta})}{dt} \cong \frac{\alpha\omega_k}{2}\left[2\theta_0^2 + 3\theta_0\boldsymbol{\delta\theta} + \boldsymbol{\delta\theta}^2\right]\boldsymbol{\delta\theta} + \gamma\mu_0\boldsymbol{h}_\phi(t). \tag{35}$$

Thus, we can see that the linearization of (33) requires that $\delta\theta \ll \theta_0$, otherwise higher order terms start to become important. (Indeed, the same approximation is required to derive (22), i.e., the W-L process for STO phase noise, as presented in Section III-A.) We shall return to this point in some detail in Section VIII, where we use numerical integration to clearly demonstrate the limitations of analytical solutions for (34).

To solve (34), one approach is to substitute a deterministic impulse function for the thermal term to determine the impulse response of the system. Given that our model for thermal field noise is a train of random impulse functions, it is then a simple extrapolation to solve for the stochastic case. Taking the Fourier transform of (34) after making the substitution $\delta(t) \to |\gamma|\mu_0\boldsymbol{h}_\phi(t)$, we obtain

$$\delta\theta(\omega) = -\frac{1}{i\omega + \eta}. \tag{36}$$

(See derivation of (115) in the Appendix for details of the general method.) From this, we obtain the spectral density for amplitude fluctuations:

$$\begin{aligned} S_{\delta\theta}^{\mathrm{OU}}(\omega) &= \frac{\alpha\omega_T}{\eta^2}\frac{1}{(\omega/\eta)^2+1} \\ &= \frac{\omega_T}{\alpha\omega_k^2 m^4}\frac{1}{(\omega/\eta)^2+1} \end{aligned} \tag{37}$$

where $m = \sin\theta_0$.

Note that the spectral density of the angular fluctuations scales inversely with the square of the restoration rate. Indeed, the restoration rate is of no less importance than the dependence of oscillator frequency Ω_0 on excitation amplitude m that has been the focus of past treatment of phase noise in STOs [9], [34]. It can be measured using the methods described in [5] and is essential to a complete understanding of how STO noise depends on physical parameters.

Now, we can compute the spectral density for the O-U phase noise by expanding (20) about steady-state:

$$\phi_2(t) = \omega_k \sin\theta_0 \int_0^t \boldsymbol{\delta\theta}(t')dt'. \tag{38}$$

Again, using standard stochastic transformation theory (Appendix, (115)), we have

$$S_\phi^{\mathrm{OU}}(\omega) = \frac{\omega_T}{\alpha(m\omega)^2}\frac{1}{(\omega/\eta)^2+1}. \tag{39}$$

The spectral density for frequency fluctuations is

$$S_\Omega^{\mathrm{OU}}(\omega) = \frac{\omega_T}{\alpha m^2}\frac{1}{(\omega/\eta)^2+1}. \tag{40}$$

Equations (39) and (40) *are central results of this paper*. We see that the frequency noise for the O-U process is no longer spectrally white, as it was for the W-L process. For $\omega \ll \eta$, the frequency noise appears spectrally white, but for $\omega \gg \eta$, the frequency noise has a $1/\omega^2$ character. Thus, the O-U process inherent in this particular component of phase noise can be thought of as a low pass filter acting on an otherwise white frequency noise source [35].

The divergence of (40) as the precession amplitude $m \to 0$ also deserves attention. Since the amplitude of excitation scales in proportion to current, as described by (29), we might surmise that this result is unphysical if the dc current is insufficient to drive steady-state dynamics. However, as stated parenthetically earlier in this section, the solution in the case of the fixed point described by (28) utilizes a stochastic equation different from that used in the derivation of (40). To proceed further, we begin with (15) and use the approximation $\sin(\theta) \cong \theta$ and $\cos(\theta) \cong 1$ for small amplitude fluctuations about the fixed point at $\theta = 0$. The resultant equation is also of the O-U form with a spectral density

$$S_\theta = \frac{\alpha\omega_T}{\nu^2}\frac{1}{(\omega/\nu)^2+1} \tag{41}$$

where $\nu \doteq |\gamma|\mu_0(\alpha(H_0+H_k) - \beta M_s)$. In this case, the variance for the polar angle θ is easily found by integrating the spectral density (see Appendix, (101)), with the result

$$\langle\boldsymbol{\theta}^2\rangle = \frac{\alpha\omega_T}{2\nu}. \tag{42}$$

As a point of validation, it can be shown that (42) is consistent with the equipartition theorem.

Since the variance for θ is non-zero at finite temperature, and θ, as a spatial coordinate, is defined only on the interval $[0, \pi]$, it must also be the case that the mean of the polar angle θ is also non-zero. To see why this is the case, we consider the properties of the stochastic variable $|\boldsymbol{\theta}|$, which is a reasonable approximation for the functional properties of the polar angle when fluctuating about the pole at $\theta = 0$. It can be shown that $\langle|\boldsymbol{\theta}|\rangle^2 = (2/\pi)\langle\boldsymbol{\theta}^2\rangle$ [36]. Thus, the average polar angle is never zero at finite temperature, implying that $m > 0$ always, and the spectral density of frequency fluctuations does not actually diverge in the limit where the current is reduced below the threshold for steady-state dynamics. In addition, and of more immediate consequence for the comparison of these theoretical results with experimental data, the approximations required in the derivation of (34) from (33) are no longer valid for sufficiently small θ_0. More will be presented on this topic in Section VIII.

Returning to (40), the fact that S_{ϕ}^{OU} is independent of anisotropy at Fourier frequencies below η deserves special mention. For the O-U phase noise to be independent of H_k appears to be inconsistent since the physical origin of this particular noise component stems from the dependence of oscillation frequency on amplitude, which is itself proportional to anisotropy. However, since the restoration rate η is also proportional to anisotropy, these two factors cancel in the final derivation of (39). The only effect that a change in anisotropy has on the phase noise is a shift of the knee frequency, where the noise spectrum changes from a 20 dB/decade to a 40 dB/decade slope.

Given that the frequency noise spectrum for the O-U process is not white, the calculation of the oscillator linewidth is not as simple as in the case of the W-L process. The next section describes in detail how the filtered white noise of the O-U process affects the phase diffusion and line shape of the oscillator.

IV. Phase Diffusion for Colored Frequency Noise

In this section we show that a frequency noise spectrum $S_{\Omega}^{\mathrm{OU}}(\omega)$ that is not constant for all ω implies a phase variance that does not grow linearly with time and a line shape that is not Lorentzian. In this case, we cannot simply identify a phase diffusion constant and linewidth with $S_{\Omega}^{\mathrm{OU}}(\omega)$, as we did for the W-L process. We therefore proceed by directly calculating the evolution of phase variance with time for a spectral density of the form in (40). We then show how the actual time evolution of phase variance affects the line shape of the oscillator.

We begin by applying the time-domain impulse-response solution $\delta\theta(t)$ to (34):

$$\delta\theta(t) = \Lambda \exp(-\eta t) \tag{43}$$

where $\Lambda = \Delta t|\gamma|\mu_0 h_0$, and h_0 is the amplitude of the thermal field pulse and Δt is the duration. To proceed further, we can conveniently first calculate the variance of the polar angle about the steady-state value. From the thermal noise model presented in Section II, and with the assumption that $\delta\theta \ll \theta_0$, we have the following equation for the initial polar angle $\delta\theta_i$ at time $t = 0$:

$$\boldsymbol{\delta\theta}_i = \sum_{n=-\infty}^{0} \boldsymbol{\Lambda}_n \exp(\eta \boldsymbol{t}_n) \tag{44}$$

where $\boldsymbol{\Lambda}_n \doteq \Delta t|\gamma|\mu_0 \boldsymbol{\delta H}_n$ and $\boldsymbol{t}_n < 0$ for $n < 0$. Note that the polar angle at a specific moment in time is the sum result of an infinite number of decaying fluctuations in the past. Of course, only those fluctuations within $\sim 1/\eta$ of $t = 0$ contribute significantly to the sum. Squaring and averaging, we obtain

$$\begin{aligned}\left\langle \boldsymbol{\delta\theta}_i^2 \right\rangle &= \lambda \int_0^{\infty} \left\langle \boldsymbol{\Lambda}_n^2 \right\rangle \exp(-2\eta t)dt \\ &= \frac{\lambda \left\langle \boldsymbol{\Lambda}_n^2 \right\rangle}{2\eta}\end{aligned} \tag{45}$$

where λ is the mean pulse rate for the Poisson process.

Now, to calculate the variance for the phase, we again resort to the thermal noise model presented in Section II, as well as (38). Using these, the O-U phase noise in the time domain may be written as

$$\begin{aligned}\boldsymbol{\phi}_2(t) = m\omega_k \Bigg[&\boldsymbol{\delta\theta}_i \int_0^t \exp(-\eta t')dt' \exp(-\eta t) \\ &+ \int_0^t \sum_{n=-\infty}^{+\infty} \boldsymbol{\Lambda}_n \exp(-\eta(t' - \boldsymbol{t}_n))\Phi(t' - \boldsymbol{t}_n)dt' \Bigg]\end{aligned} \tag{46}$$

where $\Phi(t)$ is the Heaviside step function, with $\Phi(t) = 1$ for $t > 0$ and $\Phi(t) = 0$ for $t < 0$. Integrating, we find

$$\begin{aligned}\boldsymbol{\phi}_2(t) = -\frac{m\omega_k}{\eta} \Bigg[&\boldsymbol{\delta\theta}_i (1 - \exp(-\eta t)) \\ &+ \sum_{n=0}^{\mathrm{floor}(\lambda t)} \boldsymbol{\Lambda}_n (1 - \exp(-\eta(t - \boldsymbol{t}_n))) \Bigg]\end{aligned} \tag{47}$$

where we have assumed that $\lambda t \gg 1$ and $t \gg 1/\eta$. Squaring the phase angle waveform and taking the mean, we obtain

$$\langle [\boldsymbol{\phi}_2(t)]^2 \rangle = \left(\frac{\gamma\mu_0}{\alpha m}\right)^2 \frac{S_h}{\eta}[\eta t - 1 + \exp(-\eta t)] \tag{48}$$

where we used (45), $\lambda \gg \eta$ in order to assume a uniform distribution of field fluctuations over the interval $[0, t]$, and we made use of $\lambda\langle \boldsymbol{\Lambda}_n^2 \rangle = (\gamma\mu_0)^2 S_h$, as derived from (8) and the definition of $\boldsymbol{\Lambda}_n$. Equation (48) is in agreement with that of [11], and was first derived by Ornstein in 1919 to describe the variance of position for a particle with inertia undergoing Brownian motion [32].

We see in (48) that the low pass filtering of the frequency noise in (40) for an O-U process causes the phase variance to increase as t^2 (to lowest order) for $t \ll 1/\eta$, and it eventually grows linearly in time for $t \gg 1/\eta$. Such nonlinear time evolution for the phase variance will generally result in a non-Lorentzian line shape for the phase noise limited spectrum, as was previously discussed in [11].

Determination of the oscillator power spectral line shape $\tilde{m}_x^2$ requires evaluating the following Fourier transform [30]:

$$\tilde{m}_x^2(\Omega + \Omega_0) = \int_{-\infty}^{+\infty} \exp\left(-\frac{\langle [\boldsymbol{\phi}_2(|t|)]^2 \rangle}{2}\right) \exp(-i\Omega t)dt \tag{49}$$

where $\tilde{m}_x^2$ is proportional to the Fourier transform of the power in the x-component of the magnetization, and Ω_0 is the nominal oscillator frequency. (Our choice of $\tilde{m}_x^2$ is arbitrary. We could have just as easily chosen $\tilde{m}_y^2$ with no loss of generality.) In the case of a phase variance such as that given in (48), a general analytic solution for the line shape is not available. However, we can consider limiting cases for line shape in certain approximations. In the low temperature limit of $\eta \gg (\gamma\mu_0/\alpha m)^2 S_h$, (which can be rewritten as $\omega_T \ll |\omega_k|\alpha^2 m^4$), we can approximate (49) as

$$\tilde{m}_x^2(\Omega+\Omega_0) \cong \int_{-\infty}^{+\infty} \exp\left(-\frac{1}{2}\left(\frac{\gamma\mu_0}{\alpha m}\right)^2 S_h|t|\right)\exp(-i\Omega t)dt = \frac{2}{\frac{1}{2}\frac{\omega_T}{\alpha m^2}}\frac{1}{\Omega^2+\left(\frac{1}{2}\frac{\omega_T}{\alpha m^2}\right)^2}. \quad (50)$$

Thus, the line shape for the oscillator power spectrum is approximately Lorentzian with a FWHM linewidth of

$$\Delta f_{\mathrm{LT}}^{\mathrm{OU}} \cong \frac{1}{\pi}\frac{|\gamma|k_B T}{\alpha m^2 M_s V} \quad (51)$$

$$= \frac{\Delta f^{\mathrm{WL}}}{\alpha^2}. \quad (52)$$

In the low temperature limit, we see that the linewidth inversely proportional to α^2 and m^2, it is independent of H_k, and is linear in T. Alternatively, in the high temperature limit of $\eta \ll (\gamma\mu_0/\alpha m)^2 S_h$ (or $\omega_T \gg |\omega_k|\alpha^2 m^4$), (49) can be approximated as

$$\tilde{m}_x^2(\Omega-\Omega_0) \cong \int_{0}^{+\infty} \exp\left(-\frac{1}{4}\left(\frac{\gamma\mu_0}{\alpha m}\right)^2 S_h \eta t^2\right)\exp(-i\Omega t)dt = 2\sqrt{\frac{\pi}{|\omega_k|\omega_T}}\exp\left(-\frac{\Omega^2}{|\omega_k|\omega_T}\right). \quad (53)$$

The amplitude line shape is approximately Gaussian and the power spectrum line shape has a FWHM linewidth of

$$\Delta f_{\mathrm{HT}}^{\mathrm{OU}} \cong \frac{1}{\pi}\sqrt{\ln(2)|\omega_k|\omega_T} = \frac{\sqrt{2\ln(2)}}{\pi}|\gamma|\mu_0\sqrt{\frac{|H_k|k_B T}{\mu_0 M_s V}}. \quad (54)$$

In the high temperature limit, we see that the linewidth is no longer a function of α or excitation amplitude m, it is a function of H_k, and is proportional to $\sqrt{T}$ rather than T. This is consistent with the result previously reported in [11].

Clearly, the extraction of the linewidth from experimental data for comparison with theory could be a misleading exercise for the case where $\eta \cong (\gamma\mu_0/\alpha m)^2 S_h$, because neither the low nor high temperature limits are applicable. Indeed, this is probably often the case for most experimental measurements currently undertaken [37]. For example, if we take $\alpha = 0.02, T = 300$ K, $V = 1.4\times 10^4$ nm^3 (e.g., a ~40 nm radius, 3 nm thick circular dot), $M_s = 800$ kA/m, and $H_k = -M_s$, we calculate that $\omega_T/(\alpha^2|\omega_k|) \approx 1.8$, implying that the line shape is neither Lorentzian nor Gaussian at room temperature, except at sufficiently small amplitudes ($m \lesssim 0.5$), whereupon the system is in the high-temperature limit. As a consequence, the temperature dependence of the linewidth is no longer expected to follow the simple functional forms of either (51) or (54). *Under such circumstances, a less ambiguous method for comparison with theory would be the direct measurement of oscillator phase spectral density, which would allow for comparison of experimental data with* (39).

In the low temperature limit, we note that the linear combination of the W-L and O-U processes result in a linewidth that scales linearly with temperature, with the final form given by

$$\Delta f_{\mathrm{LT}} = \frac{1}{\pi}\frac{\alpha|\gamma|k_B T}{m^2 M_s V}\left[1+\left(\frac{1}{\alpha}\right)^2\right]. \quad (55)$$

In this limiting case, the O-U noise source will clearly always dominate, because $\alpha \ll 1$ for all the materials of interest for spin torque oscillators. In the high-temperature limit, the O-U and W-L process linewidths are comparable for a sufficiently small precession amplitude m_0 given by

$$m_0 = \frac{\alpha}{\sqrt{2\ln(2)}}\sqrt{\frac{k_B T}{\mu_0 M_s H_k V}}. \quad (56)$$

If we assume physically realizable parameters that are consistent with the high-temperature limit, we find that $m_0 \ll 1$, *implying that the O-U contribution to the linewidth remains dominant even in the high-temperature limit, except for the instance of extremely small amplitude precession.*

Since we expect the W-L process to be far less important for determining oscillator linewidth, we will ignore its effect from this point forward, except as a point of comparison with previously published work.

V. Sub-Threshold Current Regime

In Section III-B, we pointed out that thermal fluctuations effectively maintain $m > 0$ as the current is reduced below threshold for steady-state dynamics. This point can be elaborated upon in the context of sub-threshold dynamics, where we can glean some insight into the nature of ferromagnetic resonance in the context of phase noise. When the dc current satisfies the condition in (28), phase noise still exists, even though the spin torque is not sufficient to drive the device into steady-state dynamics. In other words, thermal fluctuations alone maintain periodic oscillations with a non-zero amplitude. This effect is sometimes referred to as "mag noise," and has recently garnered substantial attention, because it poses a significant deliterious noise source for hard disk drives [38]–[40].

It is instructive to consider how the phase noise for the macrospin in this particular geometry scales with current when operating the STO below the threshold current. First, we make the identification that $m^2 = \langle\boldsymbol{\theta}^2\rangle$, where the variance of the polar magnetization angle is given by (42). Second, we recognize that the W-L process for phase noise is essentially unchanged in the sub-threshold regime. Finally, we utilize (15), expanding for small θ, in order to determine how small amplitude polar angle fluctuations affect the O-U contribution to the noise, exactly as was done in the derivation of (41) in the previous sub-section. Following these first two steps, we find the thermally driven W-L contribution to the linewidth is given by

$$\Delta f^{\mathrm{WL}} = \frac{\nu}{\pi} \quad (57)$$

where $\nu \doteq (\alpha\Omega_0(0) - \beta(I)\omega_M)$ (previously defined in Section III-B), $\Omega_0(0)$ is the FMR frequency (previously defined in Section III), and $\omega_M = |\gamma|\mu_0 M_s$. (Note that the threshold condition for steady-state dynamics in (28) is equivalent to $\nu = 0$.) At this point, we immediately see that the phase-noise-limited linewidth for the W-L process when $\beta = 0$ is indeed equivalent to the ferromagnetic resonance linewidth [41]. In addition, the W-L linewidth decreases linearly as current increases in the sub-threshold regime, consistent with experimental observations for nanopillars [42], leading to the notion that spin torque can be regarded as a kind of "negative damping" [3].

Now we turn to the O-U contribution to the thermally driven linewidth. Following the same steps used in the derivation of (40), but utilizing instead the sub-threshold spectral density for the polar angle fluctuation in (41), we obtain

$$S_{\Omega}^{\mathrm{OU}} = \frac{(\alpha\omega_T\omega_k)^2}{2\nu^3}\frac{1}{\left(\frac{\omega}{\nu}\right)^2 + 1}. \tag{58}$$

Following the same procedure that was outlined in Section IV, we find in the low temperature limit of $\omega_T \ll \sqrt{2}\nu^2/\alpha\omega_k$ that the O-U contribution to the linewidth is given by

$$\Delta f_{\mathrm{LT}}^{\mathrm{OU}} = \frac{1}{4\pi}\frac{(\alpha\omega_T\omega_k)^2}{2\nu^3}. \tag{59}$$

Thus, while the W-L linewidth goes to zero as the current approaches threshold from below, the O-U contribution diverges, in much the same manner that the linewidth above threshold diverges in (55) as the current approaches threshold from above. Of course, as discussed earlier in the context of phase noise at currents above threshold, this simple analysis breaks down at a sufficiently large current, for several reasons. First, the low-temperature approximation will eventually break down as $\nu \to 0$, requiring the application of the same approximations used in the derivation of (54), with the result that the oscillator line shape is expected to take on a Gaussian profile with a linewidth that is independent of excitation amplitude. Second, and more importantly, as $\nu \to 0$, the fluctuations in $\boldsymbol{\theta}$ will become sufficiently large that the approximations that are used to treat (15) as a first order stochastic differential equation will no longer be valid, requiring a numerical treatment to calculate the phase noise close to threshold. Numerical methods to determine the validity of phase noise solutions will be further discussed in Section VIII.

VI. Asymmetric Spin Torque

We now consider how the inclusion of spin torque asymmetry affects the previous equations for phase noise. While the inclusion of spin torque asymmetry is not fundamentally problematic for the case considered here, this does require some messy algebra that will not be presented. Instead, we will focus on the primary results, insofar as the inclusion of spin torque asymmetry does act to significantly reduce the phase noise and linewidth associated with the O-U process.

Various authors have proposed that the spin torque factor $\beta(I)$ in metallic nanopillars also contains an additional dependence on the relative angular orientation of the magnetization with respect to the fixed magnetic layer [3], [43]–[45] to account for the fact that the free layer also affects the spin accumulation in the nonmagnetic conductive layer between the free and the fixed layers. Such an angular dependence is used to explain why spin torque induced switching in nanopillars has an asymmetric dependence on current polarity [46], [47]. The form proposed by Slonczewski for such a dependence is [43]

$$\beta(I,\theta) = \zeta(I)g(\theta) \tag{60}$$

where

$$\zeta(I) \doteq \frac{I\hbar}{2e\mu_0 M_s^2 V} \tag{61}$$

and

$$g(\theta) = \frac{P\lambda^2}{(\lambda^2+1)+(\lambda^2-1)\cos\theta}. \tag{62}$$

In (62), P is the asymmetry of the magnetoresistance and λ is the aymmetry of the spin torque, with $\lambda = 1$ equivalent to symmetric spin torque switching, i.e., the magnitude of the switching current does not depend on the sign of the current.

Inclusion of such an asymmetry alters the results for the O-U contribution to phase noise (i.e., phase noise due to field fluctuations $\boldsymbol{h}_\phi$) in two ways. First, the polar angle for steady-state oscillations is now determined by solving the following quadratic equation:

$$\begin{aligned}0 = (\lambda^2+1)x^2 + [(\lambda^2+1) + (H_0/H_k)(\lambda^2-1)]x \\ + \left[(H_0/H_k)(\lambda^2+1) - \frac{P\lambda^2\zeta(I)M_s}{\alpha H_k}\right]\end{aligned} \tag{63}$$

where $x \doteq \cos\theta_0$, subject to the constraint $|x| \le 1$, whereby we obtain

$$\theta_0 = \arccos\left\{\frac{-B-\sqrt{B^2-4AC}}{2A}\right\} \tag{64}$$

with

$$A \doteq (\lambda^2+1), \tag{65}$$

$$B \doteq (\lambda^2+1) + (H_0/H_k)(\lambda^2-1) \tag{66}$$

$$C \doteq (H_0/H_k)(\lambda^2+1) - \frac{P\lambda^2\zeta(I)M_s}{\alpha H_k}. \tag{67}$$

The physical constraint $\theta_0 \in [0,\pi]$ implies the existence of a Hopf bifurcation [48] at the minimum current I_c, which satisfies this constraint. Second, in the limit of fluctuations sufficiently small to permit linearization of (33), we obtain

$$\frac{d(\delta\theta)}{dt} = \alpha\omega_k q(\theta_0)\sin^2\theta_0\delta\theta + |\gamma|\mu_0\boldsymbol{h}_\phi(t) \tag{68}$$

where

$$q(\theta_0) \doteq 1 - \frac{(H_0/H_k)+\cos\theta_0}{(\lambda^2+1)/(\lambda^2-1)+\cos\theta_0}. \tag{69}$$

Thus, the mode restoration rate is modified to be $\eta = \alpha\omega_k q(\theta_0)\sin^2\theta_0$, and the general form for the low temperature linewidth is now

$$\Delta f_{\mathrm{LT}}^{\mathrm{OU}} = \frac{\omega_T}{2\pi\alpha[mq(\theta_0)]^2}. \tag{70}$$

For the case of steady-state dynamics with $H_k < 0$, *we see that* $q(\theta_0) \ge 1$, *implying that the spin torque asymmetry acts to accelerate the return to steady-state after a thermal fluctuation, thereby reducing both the phase noise and the commensurate*

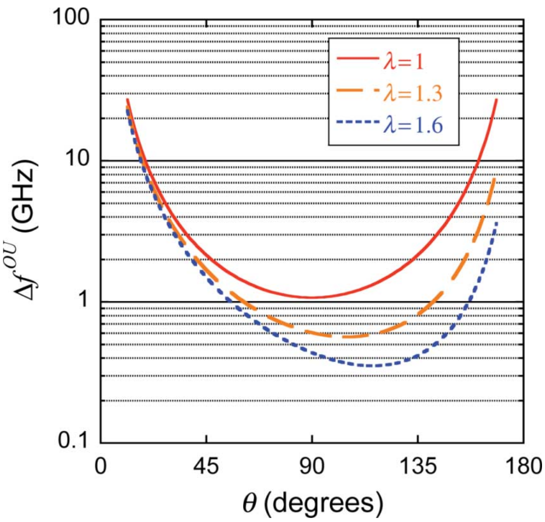

Fig. 2. Linewidth as a function of steady-state precession angle θ obtained with (70). The parameters are $\alpha = 0.02, T = 300$ K, $V = 1.4 \times 10^4$ nm^3 ellipse, $M_s = 800$ kA/m, $H_k = -M_s, H_0/H_k = -1.3$, and $\lambda = 1$ or 1.6. The red solid curve is for $\lambda = 1$, the orange dashed curve is for $\lambda = 1.3$, and the blue dotted curve is for $\lambda = 1.6$.

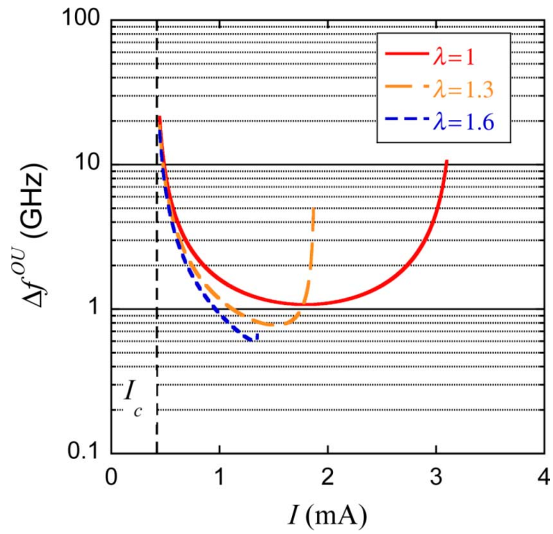

Fig. 3. Linewidth as a function of dc current obtained with both (64) and (70). Parameters used for the calculation are stated in the text. The red solid curve is for $\lambda = 1$, the dashed orange curve is for $\lambda = 1.3$, and the dotted blue curve is for $\lambda = 1.6$.

linewidth. In Fig. 2, we plot (70) as a function of steady-state angle θ_0 for the conditions $\alpha = 0.02, T = 300$ K, $V = 1.4{\times}10^4$ nm^3, $M_s = 800$ kA/m, $H_0/H_k = -1.3$, and $\lambda = 1, 1.3$, or 1.6. For the case of $\lambda = 1$, the linewidth diverges at $\theta_0 = 0, \pi$ and it has a minimum at $\theta_0 = \pi/2$. We see that the spin torque asymmetry for $\lambda = 1.6$ reduces the linewidth by a factor of anywhere from 1.3 to 8.4, depending on the steady-state angle, with increasing reductions at larger values of θ_0. The minimum linewidth is reduced by a factor of 4.5, and the minimum is shifted to a larger angle of $\theta_0 \approx 120^\circ$.

By solving (64), we can plot linewidth $\Delta f^{\rm OU}$ as a function of current with the same parameters used in Fig. 2, as well as $M_s/H_k = -1$ and $P = 1$. The results are shown in Fig. 3. While the linewidth for $\lambda = 1$ displays a "U" shaped curve, with nearly symmetric behavior about 2.1 mA, the behavior for $\lambda = 1.6$ is substantially different, with $\Delta f^{\rm OU}$ monotonically decreasing until 1.5 mA, at which point the magnetization discontinuously switches to $\theta_0 = \pi$. At its smallest value, the linewidth for $\lambda = 1.6$ is reduced by an approximate factor of 2 relative to the minimum at $\Delta f^{\rm OU} = 1.08$ GHz for $\lambda = 1$.

The magnitude of the calculated linewidths deserves further attention. As will be discussed in detail in Section X, our theoretical linewidths for smaller currents are substantially larger than those generally reported in the literature. However, there are actually scant data for the case of a near-saturation perpendicular applied field with nanopillars. What few data exist suggests that experimentally measured linewidths for the perpendicular geometry are on the order of hundreds of megahertz, which is comparable to those calculated here for $m \approx 1$. In addition, the analytical theory described by (70) breaks down for sufficiently small amplitude motion, as will be shown in Section VIII. Finally, as explained in Section III-B, thermal fluctuations establish an effective lower bound for the mean value of m. Thus, the divergence of the linewidths at small and large currents in Fig. 3 should not be construed as physically accurate.

VII. Comparison With Kim, Tiberkevich, and Slavin (KTS) Theory

Recently, the KTS theory has provided a thorough analysis of spin torque oscillator noise in the context of a specific nonlinear differential equation for spin wave modes with third-order nonlinearity in excitation amplitude [7], [9]–[11]. As such, KTS theory could be considered a more general theory than that presented here. However, while it is always possible to expand the equation for spin wave dynamics to third order in mode amplitude, quantitative comparison of the theory with experiment without fitting parameters requires detailed information concerning the particular excited spin wave mode in question. In addition, this method introduces some difficulty in extrapolating KTS theory to excitations for an arbitrarily large polar angle θ_0. For example, there exist experimental data for large amplitude excitations close to and even beyond saturation, i.e., $\theta_0 \gtrsim 1$ [49]–[51]. In this section, we analytically compare our method to the results of KTS, and we find that the equations for phase-noise limited linewidth derived by both methods agree, given a proper translation of variables between the equation of motion of the spin wave amplitude for KTS and our own equations for a macrospin dynamics in polar coordinates.

The KTS theory starts with the following equation for the complex spin wave mode amplitude [52]:

$$\frac{da}{dt} + i(\omega_0 + N|a|^2)a + \Gamma_0(1 + Q_0|a|^2)a - \Gamma_s(1 - Q_s|a|^2)a = f_n(t) \quad (71)$$

where $a = |a|\exp(-i\phi), N$ is a nonlinear frequency coefficient, Γ_0 is a linear damping coefficient, Γ_s is the linear spin torque coefficient, Q_0 is the nonlinear damping coefficient, Q_s is a nonlinear spin torque coefficient, and $f_n(t)$ is the thermal noise source term. If we make the substitution $\theta = |a|$, we can rewrite (71) as

$$\frac{d\phi}{dt} = -(\omega_0 + N\theta^2) + \frac{\mathrm{Im}[f_n(t)e^{i\phi}]}{|a|} \tag{72}$$

and

$$\frac{d\theta}{dt} = -\Gamma_0(1+Q_0\theta^2)\theta + \Gamma_s(1-Q_s\theta^2)\theta + \mathrm{Re}[f_n(t)e^{i\phi}]. \tag{73}$$

We can now see that (72) and (73) are equal to (13) and (14) in the limit of small θ, with the following equivalencies:

$$\omega_0 = |\gamma|\mu_0[H_0 + H_k] \tag{74}$$
$$\Gamma_0 = \alpha|\gamma|\mu_0[H_0 + H_k] \tag{75}$$
$$\Gamma_s = \beta(I)\omega_M \tag{76}$$
$$Q_0 = -\frac{1}{2}\frac{H_k}{[H_0 + H_k]} \tag{77}$$
$$Q_s = 0 \tag{78}$$
$$N = -\frac{1}{2}|\gamma|\mu_0 H_k. \tag{79}$$

From the KTS theory, the linewidth is calculated to be

$$\Delta f = \frac{1}{2\pi}\Gamma_0\left(\frac{k_BT}{E_0}\right)\left[1+\left(\frac{N}{\Gamma_{\mathrm{eff}}}\right)^2\right] \tag{80}$$

where E_0 is the stored energy of the oscillation and Γ_{eff} is the effective damping coefficient, defined as $\Gamma_{\mathrm{eff}} \doteq \Gamma_0(Q_s\varsigma + Q_0)$, with the supercriticality factor $\varsigma \doteq (I - I_c)/I_c$. The oscillator energy in the small amplitude limit is given by [53]

$$E_0 = \frac{\Omega_0\left(\theta_0 = 0\right) m^2 M_s V}{2|\gamma|} \tag{81}$$

where Ω_0 is the angle-dependent precession frequency defined in Section III. Using (74)–(79), and (81), we can rewrite (80) to be identical to (55). *Thus, we find that our equations for linewidth in the limit of both low temperature and small amplitude agree with that derived by KTS, with the caveat that the various linear and nonlinear coefficients in KTS theory are set by* (74) *through* (79), *as obtained from the Landau-Lifshitz-Slonczewski equation* (9).

We hasten to add that our principle motivation in this section is to show the equivalence of (55) and (80) in the limit of small amplitude oscillations near the oscillation threshold: Doing so substantiates our claim the our results are consistent with those derived by KTS. However, we recognize that (80) is a general result for oscillator linewidth near oscillation threshold that is not restricted to the particular high symmetry geometry considered here. Indeed, (80) has also been derived in [12] by a Taylor series expansion of (9) about an in-plane symmetry axis.

We note the following essential differences between our derivation of (55) and that of KTS theory. First, our derivation employs equations of motion that are derived from the LLS equation for arbitrary steady-state polar angle θ_0, whereas (71) is fundamentally based upon a third-order Taylor's series approximation that is quantitatively accurate only for $\theta_0 \lesssim 50°$. While both approaches arrive at the same final result for linewidth at low temperature and small amplitude, they differ in that our approach allows us to determine the temperature range over which the approximations used to derive (55) are valid by comparison of the analytical results with numerical solutions to (19) and (20). This will be explained in more detail in Section VIII.

There is a second essential difference between KTS and ourselves in the derivation of (55). In [9], Q_0 is not derived from a general dynamic equation such as LLS, but is instead treated as a phenomenological parameter, with an assumed value of $Q_0 = 3$. The argument to treat the damping in such a manner was first proposed in [21], where the authors suggest that the damping parameter itself is not a constant. By using such a large value for the nonlinearity in comparison to what is expected from Landau-Lifshitz in (77), the linewidths calculated using (55) were sufficiently reduced to match published data. Without adjusting the nonlinearity in such a manner, we find that the calculated linewidths tend to be 5 to 10 times greater than those measured.

VIII. Simulation Results: Limits of Linear Approximation for $d\theta/dt$

The derivation of (34), a linear equation of motion for the perturbed dynamics about steady-state, from (33), the fully nonlinear equation of motion, requires use of the approximation that the thermal fluctuations are sufficiently small to permit linearization via Taylor series expansions. Thus, it is mandatory that the range of temperatures and/or amplitudes that permit such an approximation be clearly determined before any attempt is made to compare this theory with experimental data. In other words, at a given temperature T, the approximation used to derive (34) is valid only for a sufficiently large value of θ_0. To date, this has not been adequately addressed in the literature. In this section, we demonstrate the use of numerical methods to determine the range of temperatures and amplitudes that permit linearization of (33) for a specific set of parameters. The numerical methods described here are quite elementary in nature, and should prove useful for making such determinations when these equations are used to analyze data for arbitrary experimental parameters. For the sake of simplicity, we will restrict our theoretical analysis to the low-temperature form of the linewidth given in (55).

We can numerically integrate (33) to determine the range of validity for the approximation used to derive (51). For the numerical integration, we used a time step criteria of $\delta t = 1/25\eta$, where η is the mode restoration rate, as defined in Section III-B. This ensured convergence for the numerical integration using a fourth-order Runge-Kutta fixed step method. To demonstrate that our numerical integration scheme agrees with the analytical theory, we compare in Fig. 4 the numerically calculated frequency noise spectral density S_Ω^{OU} with the theoretical prediction of (40). For sufficiently large amplitude of excitation and sufficiently small temperature, the numerical and analytical results are in excellent agreement, as will be discussed in detail

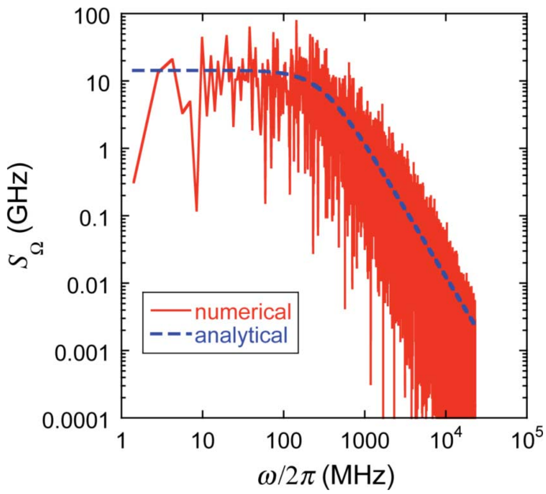

Fig. 4. Comparison of frequency noise spectrum calculated by means of analytic result and numerical integration. The dashed blue curve represents the analytical result of (51), and the red solid line is the result of numerical integration of (33). The parameters for the comparison were $T = 300$ K, $\alpha = 0.01, V = 1.4 \times 10^4$ nm^3, $H_k = -M_s$, and $m = 1$.

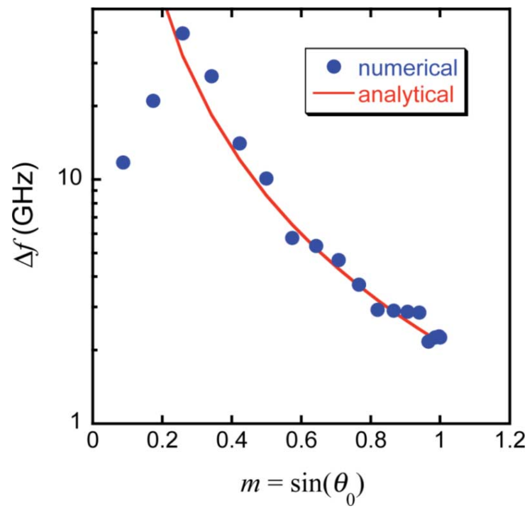

Fig. 5. Comparison of linewidth calculated by use of analytical theory and numerical integration of (33). The red curve is directly calculated from (33) and (82), as explained in the text, while the blue dots are the results of numerical integration. The parameters for the comparison were $T = 300$ K, $\alpha = 0.01, V = 1.4 \times 10^4$ nm^3, and $H_k = -M_s$.

below. (Note that the units for the frequency noise spectral density is Hz^2/Hz $=$ Hz.)

Convergence for integration of the Langevin equation was verified by checking that the numerical results were unaltered when both the noise pulse width Δt and the Poisson rate λ of the field noise pulses were varied. For the simulation results shown here, $\delta t = \Delta t$.

To numerically estimate the linewidth, we start by estimating the phase diffusion constant from the discrete time series data generated when integrating (33) over the time interval $[0, \tau]$ with a time step of δt. The generated time series data $\phi_p = \phi(p \cdot \delta t)$ form a vector of length $P = \tau/\delta t \in I^+$, which is then divided into $J \in I^+$ non-overlapping sub-series $\phi_r^j = \phi(r\cdot\delta t+(j/J)\tau)$, where $j \in [0, 1, \ldots, J-1]$ and $r \in [0.1, \ldots, (P/J)-1]$. We then calculate the time-dependent variance of the phase with the standard estimator:

$$\langle \phi^2(r \cdot \delta t)\rangle = \frac{\sum_{j=0}^{J-1}\left(\phi_r^j - \phi_0^j\right)^2}{J-1}. \tag{82}$$

We fit the resultant data with $\langle \phi^2(r \cdot \delta t)\rangle = D \cdot r \cdot \delta t$ for $r \cdot \delta t \gg 1/\eta$ to estimate the asymptotic diffusion constant at long times. The linewidth is then calculated with (26). (This particular method for determining the linewidth specifically ignores the nonlinearity in the dependence of phase variance on time, thus avoiding the complications associated with distortion of the line shape from the ideal Lorentzian form. This permits us to compare the numerical results with analytical formulae derived in earlier sections.)

In Fig. 5, we show the dependence of linewidth $\Delta f = \Delta f^{\mathrm{WL}} + \Delta f^{\mathrm{OU}}$ on excitation amplitude $m = \sin\theta$. We see that the analytic theory works well for $m > 0.2$. For excitations of smaller amplitude, the linearization of (33) that leads to (34) is no longer valid because the excursion angles at room temperature are too large to permit the small angle approximation for the expansion of the trigonometric functions in (33). We note that, while the nonlinearities in (33) appear to lead to a significant reduction in the linewidth relative to what is predicted in the analytic theory in Fig. 5, we cannot guarantee the accuracy of our numerical integration in the case when the stochastic differential equation becomes highly nonlinear. The methods for the proper integration of such equations remain a topic of ongoing research that goes well beyond the scope of this paper [29], [54].

The breakdown in the linear expansion of (33) can be graphically demonstrated in Figs. 6 and 7, where we plot the restoring torque, i.e., the right side of (33), alongside the thermal fluctuations in $\theta(t)$. Fig. 6(a) shows the time series resulting from integrating (33), while Fig. 6(b) shows the restoring torque on the horizontal axis over the same range of θ. For this large amplitude $(\mathrm{m} = 1)$ case, the linearization of (33) is clearly valid. Fig. 7 shows a small amplitude $(\mathrm{m} = 0.259)$ case where thermal fluctuations at room temperature are too large to justify the linearization of (33). The complete parameters for both cases are given in the figure captions.

The nonlinearities that affect phase noise at small amplitudes will also affect the dependence of linewidth on other parameters. For example, (55) predicts a linear dependence of linewidth on temperature. In Fig. 8(a), we see an example of such linear dependence for $m = 1$, with good agreement between the prediction of (55) and numerical simulations. However, results are very different at smaller amplitudes where the differential equation for the polar angle dynamics is no longer linear. In Fig. 8(b), we see a comparison between theory and numerics for $m = 0.34$ $(\theta_0 = 20^\circ)$. Here, we see that the temperature dependence changes slope at $T = 150$ K. Alternatively, in Fig. 8(c), at an even smaller amplitude of $m = 0.17$ $(\theta_0 = 10^\circ)$, we see that the linewidth saturates for $T > 50$ K as a result of the nonlinearity inherent in (33). Note also that the simulated linewidth for $T > 150$ K are greater than those expected from the theory for $\theta_0 = 20^\circ$, but less than those expected from the theory for $\theta_0 = 10^\circ$, reflective of the complicated manner in which the

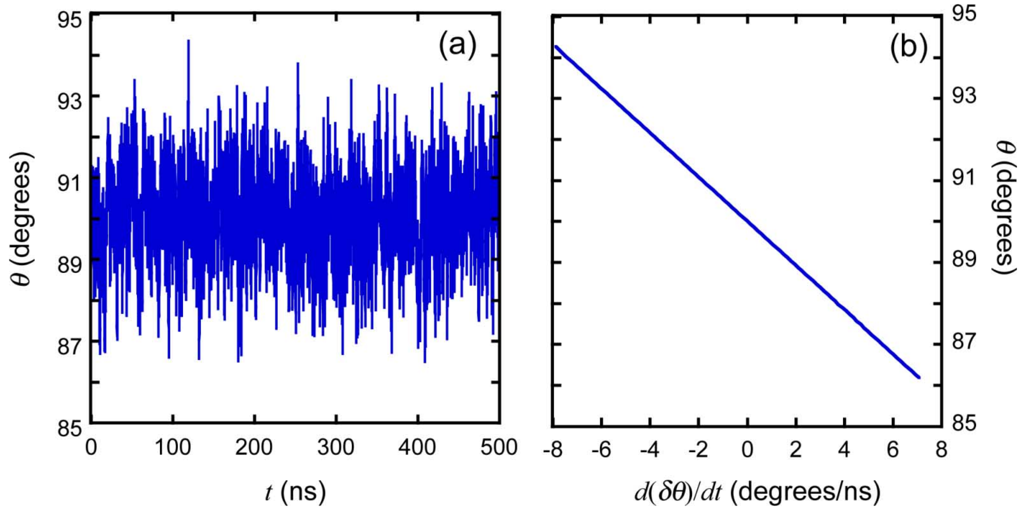

Fig. 6. Example of numerical solution of (33) for conditions where restoring torque acting on magnetization fluctuations is linear in fluctuation amplitude. Part (a) shows a sample trace of the fluctuations in the polar angle theta as a function of time. Part (b) shows how the restoring torque acting on the magnetization fluctuations behaves with varying angle. In this case, the restoring torque is clearly linear over the range of perturbations acting on the magnetization. Simulation parameters are $T = 300$ K, $\alpha = 0.01$, $V = 1.4 \times 10^4$ nm^3, $H_k = -M_s, m = 1$.

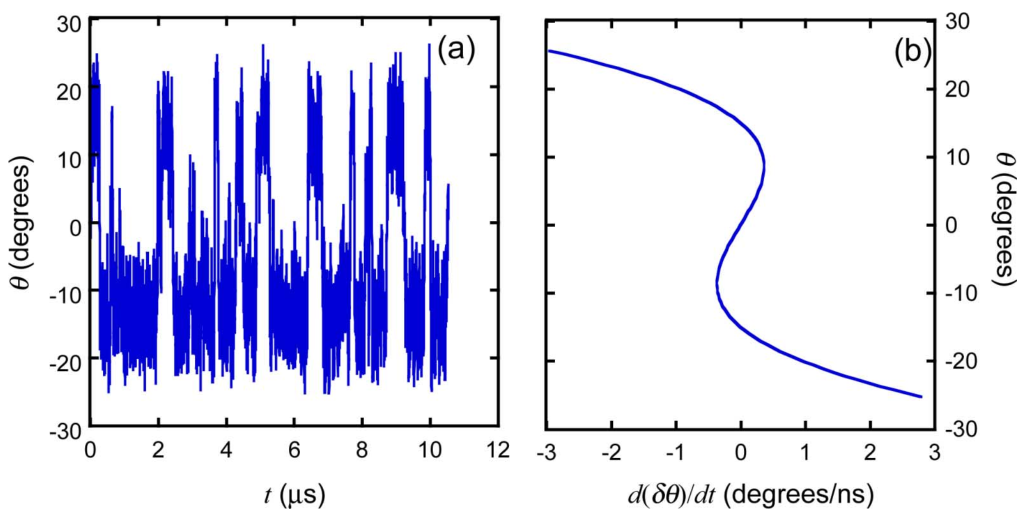

Fig. 7. Example of numerical solution of (33) for conditions where restoring torque acting on magnetization fluctuations is not linear in fluctuation amplitude. The vertical axis of part (a) includes negative polar angle values. These are physically degenerate with positive polar angles, but we use this representation to indicate events where the magnetization precession undergoes a 180° phase jump as a result of fluctuations driving the magnetization through the pole at $\theta = 0$. Simulation parameters are $T = 300$ K, $\alpha = 0.01$, $V = 1.4 \times 10^4$ nm^3, $H_k = -M_s, m = 0.259$, $(\theta_0 = 15^\circ)$.

nonlinearities of (33) affect the linewidth relative to the analytical predictions.

These results demonstrate that care must be taken when analyzing linewidth data with precession amplitudes of less than about $m = 0.4$ (at room temperature), for which nonlinearities intrinsic to the dynamics make comparison with theory problematic. Such nonlinearities may explain earlier observations of a nonlinear dependence of linewidth on temperature for steady-state oscillations in nanopillars and point-contacts [55], [56]. We stress that (13) and (14) are strictly applicable only in the case where the applied field is parallel to the anisotropy axis of the device, unlike the experiments in [55], which were conducted while a magnetic field was applied in the plane of the device. Nevertheless, we expect that the basic principle concerning nonlinear SDEs can be extended, insofar as the relevant SDE will be only approximately linear in fluctuation amplitude for a sufficiently large precession amplitude at a given temperature.

IX. Point-Contact Devices

We can extend our results to the case of point-contact structures by estimating mode volume and mode damping using the well known solution of Slonczewski [57]. In this case, the spin torque excites a mode consisting of spin waves that radiate from the point-contact into the surrounding magnetic film. We begin by assuming that the spectral density of the field noise is uncorrelated in both time and space, such that

$$\begin{aligned} C_h(\overrightarrow{\rho}, \tau) &\doteq \langle \boldsymbol{h}(\vec{r}, t)\boldsymbol{h}(\vec{r}+\vec{\rho}, t+\tau)\rangle \\ &= \frac{2\alpha k_B T}{\gamma \mu_0^2 M_s}\delta(\tau)\delta(\vec{\rho}). \end{aligned} \tag{83}$$

This assumption forms the basis for the inclusion of thermal effects in many micromagnetic simulations [58], though a rigorous theory justifying such an assumption has not yet been pre-

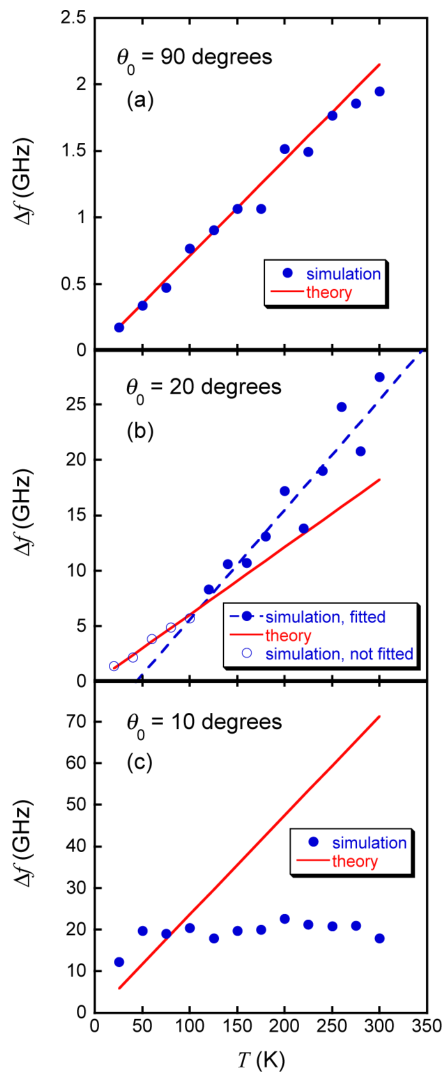

Fig. 8. Theoretical and simulated dependence of linewidth on temperature. In part (a), we show an example where the simulations based upon the numerical solution of (33) agree well with the analytical result (55). Such agreement is not the case for parts (b) and (c), where we see significant differences between theory and modeling owing to the intrinsic nonlinearity of (33), as discussed in the text. For part (b) with $\theta_0 = 20°$, the simulations agree with theory only up to a temperature of 100 K, at which point the linewidth grows faster with temperature than theory would predict. Note that linear regression of the simulation results for $T > 100$ K results in a negative intercept at $T = 0$. For part (c), we find that simulated linewidths saturate for $T > 50$ K.

sented. Nevertheless, the spectral density for the field noise is then

$$S_h(\overrightarrow{k},\omega) = \int_V \int_{-\infty}^{+\infty} C_h(\rho,\tau) \times \exp(-i\omega\tau)\exp(-i\vec{k}\cdot\vec{\rho})d\tau d^3\rho = \frac{2\alpha k_B T}{\gamma\mu_0^2 M_s}. \tag{84}$$

The point-contact is centered at the origin. We presume the existence of a spin torque excited magnetic mode $\mu(\vec{r},t) = mg(\vec{r})\exp(-i\omega t)$, where $g(0) = 1$ such that m is the mode amplitude at the origin. The normalized Fourier transform of the mode profile is

$$G(\vec{k}) = \frac{\int_V g(\vec{r})\exp(-i\vec{k}\cdot\vec{\rho})d^3r}{\max\left[\int_V g(\vec{r})\exp(-i\vec{k}\cdot\vec{\rho})d^3r\right]}. \tag{85}$$

As previously stated, a rigorous theory for the effect of spatial thermal fluctuations on eigenmodes has not yet been developed. Nevertheless, we can extend well known principles of linear response theory to estimate the spectral density for frequency fluctuations of the excited mode. Let us assume that the partial differential equation for the magnetic system allows for a Fourier transform solution $J(\vec{k},\omega)$ for a given eigenmode. Let us also assume that, under some approximation, we can factorize J into its spatial and temporal components, G and F. Now we can multiply the field noise spectral density by the temporal and spatial Fourier transform of the excited mode:

$$S_\Omega(\vec{k},\omega) = (\gamma\mu_0)^2|J(\vec{k},\omega)|^2 S_h(\vec{k},\omega) \cong |F(\omega)|^2|G(\vec{k})|^2\frac{2\alpha|\gamma|k_B T}{M_s}. \tag{86}$$

In (86), $|G(\vec{k})|^2$ acts as a spatial filter function, whereby uniformly distributed thermal fluctuations in k-space are averaged by the mode structure.

The factorization of the transfer function into spatial and temporal components presumes weak dispersion of the thermally excited spin waves. In general, this is not the case, and (86) should be considered only an approximate result for excitations near the bottom of the spin wave band, i.e., close to the ferromagnetic resonance frequency, in systems where the dipolar contribution to the dispersion is negligible.

We can now integrate (86) over all reciprocal space to obtain the spectral density of the frequency fluctuations alone:

$$S_\Omega(\omega) = \frac{1}{(2\pi)^3}\int_{V_k} S_\Omega(\vec{k},\omega)d^3k = |F(\omega)|^2\frac{2\alpha|\gamma|k_B T}{M_s V_{\rm eff}} \tag{87}$$

where

$$V_{\rm eff} = \frac{(2\pi)^3}{\int_{V_k}|G(\vec{k})|^2 d^3k}. \tag{88}$$

In the case of a point-contact spin torque oscillator, the mode at threshold is described in terms of Hankel functions, which asymptotically approach a plane wave solution far from the origin. Thus, we estimate the Fourier transform of the mode profile as

$$|G(\vec{k})|^2 \cong \frac{\kappa^2}{(k_\rho - k_0)^2 + \kappa^2} \tag{89}$$

where $\vec{k} = k_\rho\hat{\rho} + k_z\hat{z}$. Equation (89) is characteristic of an exponentially decaying plane wave radiating away from the origin, with a decay constant κ and wavenumber k_0. Integrating over reciprocal space, we obtain

$$V_{\rm eff} \cong \frac{4d\ell}{k_0} \tag{90}$$

with film thickness d and spin wave decay length $\ell \doteq 1/\kappa$.

Using the Landau-Lifshitz model for our particular geometry, the small amplitude spin wave lifetime is given by [41]

$$\tau = \frac{1}{2\alpha\Omega_0(0)}. \tag{91}$$

The spin wave decay length can be estimated by use of

$$\begin{aligned}\ell &= v_g\tau \\ &= \frac{v_g}{2\alpha\Omega_0(0)} \\ &= \frac{2Dk_0}{2\alpha\hbar(\Omega_{\rm sw}+\Omega_{\rm FMR})}\end{aligned} \tag{92}$$

where v_g is the spin wave group velocity, $\Omega_{\rm sw}$ is the spin wave frequency shift due to exchange, $\mathcal{D}$ is the spin wave exchange parameter, where $\Omega_{\rm sw} = \mathcal{D}k^2/\hbar$, and $\Omega_{\rm FMR}$ is the FMR frequency, given by $\Omega_{\rm FMR} \doteq |\gamma|\mu_0(H_0+H_k)$. From [57] we can estimate $\Omega_{\rm sw}$ at threshold to be

$$\Omega_{\rm sw} \cong 1.43\frac{\mathcal{D}}{\hbar r_\star^2} \tag{93}$$

where $r_\star$ is the nanocontact radius. Substituting (93) into (92), we obtain

$$\ell = \frac{2k_0}{2\alpha\left(\frac{1.43}{r_\star^2}+\frac{\hbar\Omega_{\rm FMR}}{\mathcal{D}}\right)}. \tag{94}$$

Substituting (94) into (90), we end up with

$$V_{\rm eff} = \frac{8d}{2\alpha\left(\frac{1.43}{r_\star^2}+\frac{\hbar\Omega_{\rm FMR}}{\mathcal{D}}\right)}. \tag{95}$$

The inverse proportionality of $V_{\rm eff}$ on α is understood in terms of the propagation distance of the mode into the surrounding magnetic medium, resulting in a substantial increase in the effective mode volume relative to the volume of the material directly under the point-contact. The significant enhancement of the mode volume suggests that we can restrict our analysis to the low temperature limit for linewidth, i.e., (70), since is it now very unlikely that $\omega_T \gg |\omega_k|\alpha^2 m^4$ for any realistic set of experimental parameters, given that ω_T scales inversely with mode volume.

By extension of the derivation of (70), the low temperature linewidth for a point-contact is given approximately by

$$\Delta f_{\rm LT}^{\rm OU} \cong \frac{2}{\pi}\frac{|\gamma|k_BT}{(mq(\theta_0))^2M_sd}\left(\frac{1.43}{r_\star^2}+\frac{\hbar\Omega_{\rm FMR}}{\mathcal{D}}\right) \tag{96}$$

where we include the effects of spin torque asymmetry. Oddly, this simple model predicts that the linewidth for a point-contact is actually independent of the damping parameter, in contrast to that for nanopillars, which is expected to have an inverse dependence on the damping parameter in the low temperature limit. We find that the inverse proportionality of the effective volume on α cancels out the proportionality of the mode restoration rate on α. If α is large, the mode restoration rate is faster, resulting in less phase noise for a given perturbation size, but the effective mode volume shrinks in such a way that the net result is unchanged.

For typical device parameters at room temperature, with $\Omega_{\rm FMR} = 20$ GHz, $\mathcal{D} = 4$ meV·nm^2, $m = 1$ (maximum amplitude), $\lambda = 1.6, \delta = 4$ nm, and $r_\star = 30$ nm, we calculate a linewidth of 32 MHz, which is on the order of linewidths measured in point-contacts with a perpendicular applied field [59].

X. Discussion

Houssameddine *et al.* recently proposed that phase and frequency noise constitute two distinct contributors to linewidth in spin torque oscillators [60]. However, as should be clear from the details of the analysis presented here, there is no distinction between frequency and phase from the perspective of oscillator noise theory. While there may be multiple physical mechanisms that contribute to oscillator phase noise, and each mechanism may have a substantially different dependence of the spectral density on Fourier frequency, *it is always the case that complete knowledge of the phase noise spectral density is sufficient to calculate the line shape of the oscillator spectrum* [4], [30], assuming that amplitude noise is negligible.

The magnitude of the predicted linewidth by use of (55) warrants further discussion. When spin torque asymmetry is taken into account, (70) predicts linewidths of 600 MHz or greater, depending on the excitation amplitude (parameters: $\alpha = 0.02, T = 300$ K, $V = 1.4\times10^4$ nm^3, $M_s = 800$ kA/m, $(H_0)/(H_k) = -1.3$, and $\lambda = 1.6$). Experimentally determined linewidths at room temperature for nanopillar spin torque oscillator devices typically range from 25 to 500 MHz, depending on the particular experimental parameters [37], [50], [51], [55], [61]–[66]. For all but one of these experimental investigations, the applied magnetic field was in the sample film plane. In [50] Kiselev *et al.*, observed room-temperature linewidths anywhere between 250 and 700 MHz when the applied perpendicular field was sufficiently large to saturate the Permalloy free layer parallel to the applied field. (The Co reference layer was canted by 30° out of the film plane.) In the same experiments, when the magnetic field was sufficiently large to saturate both the free and fixed layers parallel to the applied perpendicular field, microwave signals were no longer observed. This is to be expected, because the plane of the magnetic precession orbit is predicted to be perpendicular to the magnetization direction of the fixed layer, thereby precluding ac modulation of the device resistance via the giant magneto-resistance effect. Thus, for experimental conditions that are a practical approximation to the high-symmetry geometry considered in the present work, the scant data are at least within the same magnitude as the predictions of our thermal noise theory at large amplitudes $(m \lesssim 1)$.

For experiments with an in-plane orientation of the applied magnetic field, we expect significantly narrower linewidths than those predicted by the theory presented here. *This can be understood in terms of the basic process that underlies the O-U source of phase noise: Due to the ellipicity of the precessional orbit,* *the effective damping rate for the in-plane geometry is significantly larger than that for the perpendicular geometry* [41] , *implying that the restoration rate is also faster*. Since the phase noise is, in general, inversely proportional to the restoration rate (because phase fluctuations are proportional to the time integral of the frequency fluctuations,) we expect that in-plane experiments will usually yield much narrower linewidths than for the case of a perpendicular applied field.

The functional forms of the phase noise spectral densities in (23) and (39) present the opportunity to experimentally distinguish between the different sources of phase noise. In particular, the occurrence of a knee frequency in the spectral density predicted by (39) should be easily detected using conventional phase noise measurement techniques. For example, if $\alpha = 0.01$, $\mu_0 H_k = -25$ mT, and $m = 0.5$, the knee frequency in the phase noise is expected to occur at 11 MHz, which is easily measured with existing methods [5]. The occurrence of a low frequency knee in the phase noise would be a distinguishing feature of phase noise that results from amplitude fluctuations.

The predictions made here for phase noise have implications for applications of STOs. Practical digital and communication applications require a phase noise figure typically in the range of -100 dBc/Hz for 1 MHz offsets [67], [68], where we define the phase noise figure in terms of the one-sided phase-noise spectral density given in (118) of the Appendix. (Such a value for phase noise is equivalent to a phase-noise limited generation linewidth of approximately 1 kHz, assuming the phase noise is purely diffusive in character.) Using (39), (118), and including the effects of spin torque asymmetry ($\lambda = 1.6$), the minimum predicted phase noise figure is on the order of -42 dBc/Hz at 1 MHz offset when the same parameters are used as those in the generation of Fig. 2. Thus, the phase noise for a STO in this particular geometry, i.e., a nanopillar that behaves like a macrospin in a perpendicular applied field, will probably always be considered unacceptable for the vast majority of practical applications. Even with a material that exhibits damping larger by an order of magnitude, the noise figure would be improved by only 10 dB. For a point-contact with the parameters used in Section IX, the larger effective mode volume should have some benefit, but the phase noise is reduced again by only 10 dB, with a minimum of approximately -58 dBc/Hz at a 1 MHz offset. Use of material of low anisotropy does not change the low frequency phase noise, as mentioned in Section III-B, but it does shift the knee frequency for the phase noise spectrum to lower frequencies. The knee frequency could be pushed down to a few megahertz by use of very low anisotropy materials. If we ignore spin torque asymmetry, we could possibly achieve a phase noise as low as almost -87 dBc/Hz at a 10 MHz offset by use of a material with $\mu H_k = -1$ mT. However, if we include spin torque asymmetry ($\lambda = 1.6$) and assume an applied field of $\mu_0 H_0 = 1$ T (as required for high frequency operation), any advantage associated with reduced anisotropy is eliminated, and the resultant phase noise is -62 dBc/Hz at a 10 MHz offset.

We are therefore led to the conclusion that there are no obvious means (as indicated by the simple theory presented here) to substantially reduce phase noise in spin torque oscillators in this particular geometry of high-symmetry to make them competitive for most microwave applications. Of course, substantial data exist to the effect that linewidths can be much narrower than what are predicted here, simply by working in a low symmetry geometry where the applied field is in the plane of the nanopillar. Indeed, room-temperature linewidths on the order of 10 MHz have been reported on several occassions [63], [64], [66]. As mentioned above, the dependence of linewidth on the polar applied field angle can be partially explained in terms of the dependence of the restoration rate on the ellipticity of the precessional orbit, where a highly elliptical orbit should also exhibit an enhanced restoration rate. In addition, enhanced spin torque asymmetry (see Section VI) can lead to further line shape narrowing. However, even a linewidth of 1 MHz is still three orders of magnitude too broad for practical consideration, and a clear path for further reductions of phase noise remains elusive.

APPENDIX I

To provide a proper model of phase noise in a linear system, it is useful to review basic properties of stochastic processes and how phase noise can be calculated based upon knowledge of the fundamental noise processes involved. Much of the material found here is based upon an excellent review of Gaussian stochastic processes found in [31]. We will indicate random variables in bold type.

The autocovariance function for a time-evolving random variable $\boldsymbol{x}(t)$ is defined as

$$C_x(t_1, t_2) \doteq \langle [\boldsymbol{x}(t_1) - \langle \boldsymbol{x}(t_1) \rangle][\boldsymbol{x}(t_2) - \langle \boldsymbol{x}(t_2) \rangle] \rangle \tag{97}$$

where the average is taken with respect to all possible realizations of the random process. If $\boldsymbol{x}(t)$ is a stationary process of zero mean, then we obtain the autocorrelation function

$$C_x(\tau) = \langle \boldsymbol{x}(t) \boldsymbol{x}(t+\tau) \rangle. \tag{98}$$

The spectral density for $\boldsymbol{x}(t)$ is defined as

$$S_x(\omega) \doteq \int_{-\infty}^{+\infty} C_x(\tau) e^{-i\omega\tau} d\tau \tag{99}$$

with a self-consistent inverse transform relationship

$$C_x(\tau) = \frac{1}{2\pi} \int_{-\infty}^{+\infty} S_x(\omega) e^{i\omega\tau} d\omega. \tag{100}$$

The variance of $\boldsymbol{x}(t)$ is defined as

$$\langle \boldsymbol{x}^2 \rangle \doteq C_x(0) \tag{101}$$

$$= \frac{1}{2\pi} \int_{-\infty}^{+\infty} S_{\boldsymbol{x}}(\omega) d\omega. \tag{102}$$

Suppose that the autocovariance function for $\boldsymbol{x}(t)$ has the following form:

$$C_x(\tau) = c_x \delta(\tau). \tag{103}$$

In this case, the noise is said to be "white", with a flat spectral density, such that

$$S_x = c_x \int_{-\infty}^{+\infty} \delta(\tau) e^{-i\omega\tau} d\tau \tag{104}$$
$$= c_x. \tag{105}$$

A generalized, constant amplitude oscillatory signal $f(t)$ may be written as

$$f(t) = F \sin(\Phi(t)) \tag{106}$$

where the instantaneous angular frequency $w(t)$ is defined as [69]

$$w(t) \doteq \frac{d\Phi}{dt}. \tag{107}$$

Now, we can introduce a noisy component of the frequency (or, equivalently, the phase) into our oscillator. The instantaneous frequency $\boldsymbol{w}(t)$ and phase $\boldsymbol{\Phi}(t)$ are to be considered stochastic quantities, with the relationship

$$\boldsymbol{w}(t) = \frac{d\boldsymbol{\Phi}}{dt}$$
$$= \Omega_0 + \boldsymbol{\Omega}(\tau) \tag{108}$$

where Ω_0 is the mean of the frequency and $\boldsymbol{\Omega}(t)$ is the zero mean component of the frequency noise. Equivalently, the instantaneous phase for such a noisy oscillator may be written as

$$\boldsymbol{\Phi}(t) = \int_0^t (\Omega_0 + \boldsymbol{\Omega}(\tau)) d\tau$$
$$= \Omega_0 t + \boldsymbol{\phi}(t) \tag{109}$$

where

$$\boldsymbol{\phi}(t) \doteq \int_0^t \boldsymbol{\Omega}(\tau) d\tau. \tag{110}$$

The oscillator output is therefore

$$f(t) = F \sin(\boldsymbol{\Phi}(t))$$
$$= F \sin(\Omega_0 t + \boldsymbol{\phi}(t)). \tag{111}$$

The phase is the most important figure of merit for oscillator performance. In fact, once the total phase has been fully characterized, it is possible to derive all other quantities associated with the oscillator [4]. The phase noise is essentially a measure of the stability of the oscillator, and once we know the phase noise, we can specify the accuracy of a clock based upon the oscillator, and how that accuracy degrades with operational time.

Let us suppose that the oscillator frequency is deterministically related to quantity x in the time domain via the following linear differential equation:

$$\sum_{k=0}^{n} A_k \frac{d^k \Omega}{dt^k} = \sum_{j=0}^{m} B_j \frac{d^j x}{dt^j}. \tag{112}$$

The complementary relation in frequency space is

$$\tilde{\Omega}(\omega) = \mathcal{H}(\omega) \tilde{x}(\omega) \tag{113}$$

where the transfer function $\mathcal{H}(\omega)$ is given by

$$\mathcal{H}(\omega) = \frac{\sum_{j=0}^{m} B_j (i\omega)^j}{\sum_{k=0}^{n} A_k (i\omega)^k}. \tag{114}$$

If we now allow $\boldsymbol{x}$ to be a random variable derived from a stationary process, we can use linear response theory to relate the spectral density for frequency noise to the spectral density of $\boldsymbol{x}$ as

$$S_\Omega(\omega) = |\mathcal{H}(\omega)|^2 S_x(\omega). \tag{115}$$

Similarly, from (110), we know that the spectral density for the phase noise is related to the spectral density of the frequency noise as

$$S_\phi(\omega) = \frac{1}{\omega^2} S_\Omega(\omega). \tag{116}$$

Combining (115) and (116), we obtain the spectral density for the phase noise in terms of the spectral density of $\boldsymbol{x}$:

$$S_\phi(\omega) = \frac{|\mathcal{H}(\omega)|^2}{\omega^2} S_x(\omega). \tag{117}$$

We note that the spectral density for phase noise is usually specified in the literature in terms of the single-sideband spectral purity function $\mathcal{L}(\omega)$, defined as

$$\mathcal{L}(\omega) = 10 \log_{10} [S_\phi(\omega) \cdot \text{ Hz}] \tag{118}$$

which is usually attributed as having the dubious units of "dBc/Hz", though it is in reality a dimensionless quantity.

From (101) and (115), the variance of the frequency noise is

$$\langle \boldsymbol{\Omega}^2 \rangle = \frac{1}{2\pi} \int_{-\infty}^{+\infty} |\mathcal{H}(\omega)|^2 S_x(\omega) d\omega. \tag{119}$$

Generally speaking, we may assume that frequency noise is a stationary process. In that case, phase noise cannot be a stationary process because it is defined in terms of the integral of frequency noise [33]. As such, we are not allowed to invoke (101) as a means to calculate the phase variance. Instead we must rely on the original definition of variance to calculate the time evolution of the phase variance correctly:

$$\langle \boldsymbol{\phi}^2 \rangle = \left\langle \left[\int_0^t \boldsymbol{\Omega}(\tau) d\tau \right]^2 \right\rangle$$
$$= \int_0^t \int_0^t \langle \boldsymbol{\Omega}(\tau_1) \boldsymbol{\Omega}(\tau_2) \rangle d\tau_1 d\tau_2$$
$$= \int_0^t \int_0^t C_\Omega(\tau_1 - \tau_2) d\tau_1 d\tau_2. \tag{120}$$

If the frequency noise is white, we have (cf. (103))

$$\begin{aligned}\langle \boldsymbol{\phi}^2 \rangle &= D \int_0^t \int_0^t \delta(\tau_1 - \tau_2) d\tau_1 d\tau_2 \\ &= D \int_0^t d\tau_1 \\ &= Dt \end{aligned} \tag{121}$$

where D is sometimes referred to as the phase diffusion constant. Thus, the mean square phase deviation, like the mean square displacement for a random walk, grows linearly in time rather than approaching a constant as for a stationary process. Note that $D = S_\Omega$ from (103) and (104), so the diffusion constant for the random walk of oscillator phase is simply the spectral density of fluctuations in oscillator frequency. Furthermore, it can be shown that the phase diffusion in (121) results in a Lorentzian spectral peak for the oscillator in the frequency domain with a linewidth [30]

$$\Delta f = \frac{D}{2\pi} \tag{122}$$

where Δf is the full-width at half-maximum (FWHM) of the peak. (When an oscillator is measured using a spectrum analyzer, there may be an additional contribution to linewidth due to amplitude fluctuations. This is commonly ignored because in applications it can be removed by following the oscillator with a saturating amplifier.) When the frequency noise is not white, (121) and (122) do not hold, as described in Section IV.

Acknowledgment

The authors wish to express their sincere gratitude to M. Pufall, M. Hoefer, B. Rippard, and S. Russek for very helpful discussions and constructive feedback on the content of the manuscript. The authors are particularly indebted to C. Nelson of the NIST Time and Frequency Division for providing very helpful tutorials on the topic of phase noise.

References

[1] J. A. Katine and E. E. Fullerton, "Device implications of spin-transfer torques," *J. Magn. Magn. Mater.*, vol. 320, no. 7, pp. 1217–1226, Apr. 2008.

[2] T. J. Silva and W. H. Rippard, "Developments in nano-oscillators based upon spin-transfer point-contact devices," *J. Magn. Magn. Mater.*, vol. 320, no. 7, pp. 1260–1271, Apr. 2008.

[3] D. C. Ralph and M. D. Stiles, "Spin transfer torques," *J. Magn. Magn. Mater.*, vol. 320, no. 7, pp. 1190–1216, Apr. 2008.

[4] S. R. Stein, "Frequency and time—Their measurement and characterization," in *Precision Frequency Control*, E. A. Gerber and A. Ballato, Eds. New York: Academic, 1985, vol. 2, ch. 12, pp. 191–231.

[5] M. W. Keller, A. B. Kos, T. J. Silva, W. H. Rippard, and M. R. Pufall, "Time domain measurement of phase noise in a spin torque oscillator," *Appl. Phys. Lett.*, vol. 94, no. 19, p. 193105, 2009.

[6] J.-V. Kim, "Stochastic theory of spin-transfer oscillator linewidths," *Phys. Rev. B*, vol. 73, no. 17, p. 174412, 2006.

[7] V. Tiberkevich, A. Slavin, and J.-V. Kim, "Microwave power generated by a spin-torque oscillator in the presence of noise," *Appl. Phys. Lett.*, vol. 91, no. 19, p. 192506, Nov. 2007.

[8] K. Mizushima, K. Kudo, and R. Sato, "Phase and amplitude noise spectra in spin-transfer nano-oscillators," *J. Appl. Phys.*, vol. 101, no. 11, p. 113903, 2007.

[9] J.-V. Kim, V. Tiberkevich, and A. N. Slavin, "Generation linewidth of an auto-oscillator with a nonlinear frequency shift: Spin-torque nano-oscillator," *Phys. Rev. Lett.*, vol. 100, no. 1, p. 017207, Jan. 2008.

[10] J.-V. Kim, Q. Mistral, C. Chappert, V. S. Tiberkevich, and A. N. Slavin, "Line shape distortion in a nonlinear auto-oscillator near generation threshold: Application to spin-torque nano-oscillators," *Phys. Rev. Lett.*, vol. 100, no. 16, p. 167201, Apr. 2008.

[11] V. S. Tiberkevich, A. N. Slavin, and J.-V. Kim, "Temperature dependence of nonlinear auto-oscillator linewidths: Application to spin-torque nano-oscillators," *Phys. Rev. B*, vol. 78, no. 9, p. 092401, Sep. 2008.

[12] K. Kudo, T. Nagasawa, R. Sato, and K. Mizushima, "Amplitude-phase coupling in a spin-torque nano-oscillator," *J. Appl. Phys.*, vol. 105, no. 7, p. 07D105, 2009.

[13] W. F. Brown, "Thermal fluctuations of a single-domain particle," *Phys. Rev.*, vol. 130, no. 5, pp. 1677LP–1686, 1963.

[14] C. W. Gardiner, , H. Haken, Ed., *Handbook of Stochastic Methods*, ser. Springer Series in Synergetics, 3rd ed. Berlin/Heidelberg: Springer-Verlag, 2004.

[15] A. Slavin and V. Tiberkevich, "Nonlinear auto-oscillator theory of microwave generation by spin-polarized current," *IEEE Trans. Magn.*, vol. 45, no. 4, pp. 1875–1918, Apr. 2009.

[16] G. Bertotti, I. D. Mayergoyz, and C. Serpico, "Analysis of random Landau-Lifshitz dynamics by using stochastic processes on graphs," *J. Appl. Phys.*, vol. 99, no. 8, p. 08F301, 2006.

[17] C. Serpico, G. Bertotti, I. D. Mayergoyz, M. d'Aquino, and R. Bonin, "Thermal stability in spin-torque-driven magnetization dynamics," *J. Appl. Phys.*, vol. 99, no. 8, p. 08G505, 2006.

[18] J. M. Shaw, T. J. Silva, M. L. Schneider, and R. D. McMichael, "Spin dynamics and mode structure in nanomagnet arrays: Effects of size and thickness on linewidth and damping," *Phys. Rev. B*, vol. 79, no. 18, p. 184404, 2009.

[19] R. E. Arias and D. L. Mills, "Dipole-exchange spin waves in perpendicularly magnetized discs: Role of the Oersted field," *Phys. Rev. B*, vol. 75, no. 21, 2007.

[20] M. A. Hoefer, T. J. Silva, and M. D. Stiles, "Model for a collimated spin-wave beam generated by a single-layer spin torque nanocontact," *Phys. Rev. B*, vol. 77, no. 14, p. 144401, 2008.

[21] V. Tiberkevich and A. Slavin, "Nonlinear phenomenological model of magnetic dissipation for large precession angles: Generalization of the Gilbert model," *Phys. Rev. B*, vol. 75, no. 1, Jan. 2007.

[22] D. A. Garanin and O. Chubykalo-Fesenko, "Thermal fluctuations and longitudinal relaxation of single-domain magnetic particles at elevated temperatures," *Phys. Rev. B*, vol. 70, no. 21, p. 212409, 2004.

[23] D. A. Garanin, "Fokker-Planck and Landau-Lifshitz-Bloch equations for classical ferromagnets," *Phys. Rev. B*, vol. 55, no. 5, pp. 3050–3057, 1997.

[24] N. Smith, "Tensor damping in metallic magnetic multilayers," *Phys. Rev. B*, vol. 80, no. 6, p. 064412, 2009.

[25] J. Foros, A. Brataas, G. E. W. Bauer, and Y. Tserkovnyak, "Noise and dissipation in magnetoelectronic nanostructures," *Phys. Rev. B*, vol. 79, no. 21, p. 214407, 2009.

[26] J. C. Slonczewski, "Current-driven excitation of magnetic multilayers," *J. Magn. Magn. Mater.*, vol. 159, no. 1–2, pp. L1–L7, 1996.

[27] Y. Tserkovnyak, A. Brataas, and G. E. W. Bauer, "Spin pumping and magnetization dynamics in metallic multilayers," *Phys. Rev. B*, vol. 66, no. 22, pp. 224 403–224 410, 2002.

[28] M. D. Stiles, J. Xiao, and A. Zangwill, "Phenomenological theory of current-induced magnetization precession," *Phys. Rev. B*, vol. 69, p. 054408, 2004.

[29] P. E. Kloeden and E. Platen, , I. Karatzas and M. Yor, Eds., *Numerical Solutions of Stochastic Differential Equations*, ser. Applications of Mathematics: Stochastic Modelling and Applied Probability. Berlin, Germany: Springer-Verlag, 1992, vol. 23.

[30] A. Blaquiere, *Nonlinear System Analysis.*. New York: Academic, 1966.

[31] C. W. Helstrom, *Probability and Stochastic Processes for Engineers.*. New York: Macmillan, 1984.

[32] G. E. Uhlenbeck and L. S. Ornstein, "On the theory of the Brownian motion," *Phys. Rev.*, vol. 36, no. 5, pp. 823–841, Sep. 1930.

[33] D. T. Gillespie, "The mathematics of Brownian motion and Johnson noise," *Amer. J. Phys.*, vol. 64, no. 3, pp. 225–240, 1996.

[34] B. Georges, J. Grollier, V. Cros, A. Fert, A. Fukushima, H. Kubota, K. Yakushijin, S. Yuasa, and K. Ando, "Origin of the spectral linewidth in nonlinear spin-transfer oscillators based on MgO tunnel junctions," *Phys. Rev. B*, vol. 80, no. 6, p. 060404, 2009.

[35] E. Bibbona, G. Panfilo, and P. Tavella, "The Ornstein-Uhlenbeck process as a model of a low pass filtered white noise," *Metrologia*, vol. 45, pp. S117–S126, 2008.

[36] M. Hoefer and J. Harlim, private communication, Sep. 2009.

[37] C. Boone, J. A. Katine, J. R. Childress, J. Zhu, X. Cheng, and I. N. Krivorotov, "Experimental test of an analytical theory of spin-torque-oscillator dynamics," *Phys. Rev. B*, vol. 79, no. 14, p. 140404, 2009.

[38] N. Smith and P. Arnett, "White-noise magnetization fluctuations in magnetoresistive heads," *Appl. Phys. Lett.*, vol. 78, no. 10, pp. 1448–1450, 2001.

[39] N. Stutzke, S. L. Burkett, and S. E. Russek, "Temperature and field dependence of high-frequency magnetic noise in spin valve devices," *Appl. Phys. Lett.*, vol. 82, no. 1, pp. 91–93, 2003.

[40] N. Smith, "Micromagnetic modeling of magnoise in magnetoresistive read sensors," *J. Magn. Magn. Mater.*, vol. 321, no. 6, pp. 531–538, 2009.

[41] V. Kambersky and C. E. Patton, "Spin-wave relaxation and phenomenological damping in ferromagnetic-resonance," *Phys. Rev. B*, vol. 11, no. 7, pp. 2668–2672, 1975.

[42] G. D. Fuchs, J. C. Sankey, V. S. Pribiag, L. Qian, P. M. Braganca, A. G. F. Garcia, E. M. Ryan, Z.-P. Li, O. Ozatay, D. C. Ralph, and R. A. Buhrman, "Spin-torque ferromagnetic resonance measurements of damping in nanomagnets," *Appl. Phys. Lett.*, vol. 91, p. 062507, 2007.

[43] J. C. Slonczewski, "Current and torques in metallic magnetic multilayers," *J. Magn. Magn. Mater.*, vol. 247, pp. 324–338, 2002.

[44] A. A. Kovalev, A. Brataas, and G. E. W. Bauer, "Spin transfer in diffusive ferromagnet—Normal metal systems with spin-flip scattering," *Phys. Rev. B*, vol. 66, no. 22, pp. 224 424–224 428, 2002.

[45] J. Xiao, A. Zangwill, and M. D. Stiles, "Boltzmann test of Slonczewski's theory of spin-transfer torque," *Phys. Rev. B*, vol. 70, no. 17, p. 172405, Nov. 2004.

[46] D. Lacour, J. A. Katine, N. Smith, M. J. Carey, and J. R. Childress, "Thermal effects on the magnetic-field dependence of spin-transfer-induced magnetization reversal," *Appl. Phys. Lett.*, vol. 85, no. 20, pp. 4681–4683, 2004.

[47] R. Lehndorff, M. Buchmeier, D. E. Buergler, A. Kakay, R. Hertel, and C. M. Schneider, "Asymmetric spin-transfer torque in single-crystalline Fe/Ag/Fe nanopillars," *Phys. Rev. B*, vol. 76, no. 21, Dec. 2007.

[48] G. Bertotti, C. Serpico, I. D. Mayergoyz, A. Magni, M. d'Aquino, and R. Bonin, "Magnetization switching and microwave oscillations in nanomagnets driven by spin-polarized currents," *Phys. Rev. Lett.*, vol. 94, no. 12, p. 127206, 2005.

[49] W. H. Rippard, M. R. Pufall, S. Kaka, S. E. Russek, and T. J. Silva, "Direct-current induced dynamics in $Co_{90}Fe_{10}/Ni_{80}Fe_{20}$ point contacts," *Phys. Rev. Lett.*, vol. 92, no. 2, p. 027201, 2004.

[50] S. I. Kiselev, J. C. Sankey, I. N. Krivorotov, N. C. Emley, M. Rinkoski, C. Perez, R. A. Buhrman, and D. C. Ralph, "Current-induced nanomagnet dynamics for magnetic fields perpendicular to the sample plane," *Phys. Rev. Lett.*, vol. 93, no. 3, p. 036601, Jul. 2004.

[51] I. Krivorotov, N. Emley, J. Sankey, S. Kiselev, D. Ralph, and R. Buhrman, "Time-domain measurements of nanomagnet dynamics driven by spin-transfer torques," *Science*, vol. 307, no. 5707, pp. 228–231, Jan. 2005.

[52] J.-V. Kim, V. Tiberkevich, and A. N. Slavin, "Generation linewidth of an auto-oscillator with a nonlinear frequency shift: Spin-torque nano-oscillator," Jun. 2007, arXiv:cond-mat/0703317v2.

[53] M. Sparks, *Ferromagnetic-Relaxation Theory.*. New York: McGraw-Hill, 1964.

[54] D. J. Higham, "An algorithmic introduction to numerical simulation of stochastic differential equations," *SIAM Rev.*, vol. 43, no. 3, pp. 525–546, 2001.

[55] J. C. Sankey, I. N. Krivorotov, S. I. Kiselev, P. M. Braganca, N. C. Emley, R. A. Buhrman, and D. C. Ralph, "Mechanisms limiting the coherence time of spontaneous magnetic oscillations driven by dc spin-polarized currents," *Phys. Rev. B*, vol. 72, no. 22, p. 224427, 2005.

[56] M. L. Schneider, W. H. Rippard, M. R. Pufall, T. Cecil, T. J. Silva, and S. E. Russek, "Temperature dependence of spin-torque driven self-oscillations," *Phys. Rev. B*, vol. 80, p. 144412, 2009.

[57] J. C. Slonczewski, "Excitation of spin waves by an electric current," *J. Magn. Magn. Mater.*, vol. 195, no. 2, pp. L261–L268, 1999.

[58] J.-G. Zhu, "Thermal magnetic noise and spectra in spin valve heads," *J. Appl. Phys.*, vol. 91, no. 10, pp. 7273–7275, May 2002.

[59] W. H. Rippard, M. R. Pufall, and S. E. Russek, "Comparison of frequency, linewidth, and output power in measurements of spin-transfer nanocontact oscillators," *Phys. Rev. B*, vol. 74, p. 224409, 2006.

[60] D. Houssameddine, U. Ebels, B. Dieny, K. Garello, J.-P. Michel, B. Delaet, B. Viala, M.-C. Cyrille, J. A. Katine, and D. Mauri, "Temporal coherence of MgO based magnetic tunnel junction spin torque oscillators," *Phys. Rev. Lett.*, vol. 102, no. 25, p. 257202, 2009.

[61] S. I. Kiselev, J. C. Sankey, I. N. Krivorotov, N. C. Emley, R. J. Schoelkopf, R. A. Buhrman, and D. C. Ralph, "Microwave oscillations of a nanomagnet driven by a spin-polarized current," *Nature*, vol. 425, no. 6956, pp. 380–383, 2003.

[62] M. Covington, M. AlHajDarwish, Y. Ding, A. Rebei, G. Parker, N. Gokemeijer, and M. Seigler, "Spin transfer effects in current perpendicular to the plane spin valves," *J. Magn. Magn. Mater.*, vol. 287, pp. 325–332, 2005.

[63] S. I. Kiselev, J. C. Sankey, I. N. Krivorotov, N. C. Emley, A. G. F. Garcia, R. A. Buhrman, and D. C. Ralph, "Spin-transfer excitations of Permalloy nanopillars for large applied currents," *Phys. Rev. B*, vol. 72, no. 6, p. 064430, 2005.

[64] Q. Mistral, J.-V. Kim, T. Devolder, P. Crozat, C. Chappert, J. A. Katine, M. J. Carey, and K. Ito, "Current-driven microwave oscillations in current perpendicular-to-plane spin-valve nanopillars," *Appl. Phys. Lett.*, vol. 88, no. 19, p. 192507, 2006.

[65] K. V. Thadani, G. Finocchio, Z.-P. Li, O. Ozatay, J. C. Sankey, I. N. Krivorotov, Y.-T. Cui, R. A. Buhrman, and D. C. Ralph, "Strong linewidth variation for spin-torque nano-oscillators as a function of in-plane magnetic field angle," *Phys. Rev. B*, vol. 78, no. 2, p. 024409, 2008.

[66] H. Suzuki, H. Endo, T. Nakamura, T. Tanaka, M. Doi, S. Hashimoto, H. N. Fuke, M. Takagishi, H. Iwasaki, and M. Sahashi, "Characteristics of microwave oscillations induced by spin transfer torque in a ferromagnetic nanocontact magnetoresistive element," *J. Appl. Phys.*, vol. 105, no. 7, p. 07D124, 2009.

[67] A. Hajimiri, S. Limotyrakis, and T. Lee, "Jitter and phase noise in ring oscillators," *IEEE J Solid-State Circuits*, vol. 34, no. 6, pp. 790–804, June 1999.

[68] A. Hajimiri, S. Limotyrakis, and T. Lee, "Phase noise in multi-gigahertz CMOS ring oscillators," in *Proc. IEEE Custom Integrated Circuits Conf.*, May 1998, pp. 49–52.

[69] L. Cohen, *Time-Frequency Analysis: Theory and Applications.*. Englewood Cliffs, NJ: Prentice Hall PTR, 1994.